Ecology, 97(8), 2016, pp. 2125–2135
© 2016 by the Ecological Society of America

Intraspecific leaf chemistry drives locally accelerated ecosystem function in aquatic and terrestrial communities

Sara L. Jackrel,[1] Timothy C. Morton, and J. Timothy Wootton

Department of Ecology and Evolution, The University of Chicago, 1101 East 57th St., Chicago, Illinois 60637 USA

Abstract. Resource patchiness influences consumer foraging, movement, and physiology. Fluxes across ecosystem boundaries can extend these effects to otherwise distinct food webs. Intraspecific diversity of these cross-ecosystem subsidies can have large consequences for recipient systems. Here, we show intraspecific variation in leaf defensive chemistry of riparian trees drives local adaptation among terrestrial and riverine decomposers that consume shed leaf litter. We found extensive geographic structuring of ellagitannins, diarylheptanoids, and flavonoids in red alder trees. Ellagitannins, particularly those with strong oxidative activity, drive aquatic leaf decomposition. Further, spatial variation in these leaf components drives local ecological matching: in experiments using artificial food sources distinguished only by the chemical content of individual trees, we found decomposers both on land and in rivers more quickly consumed locally derived food sources. These results illustrate that terrestrial processes can change the chemistry of cross-ecosystem subsidies in ways that ultimately alter ecosystem function in donor and recipient systems.

Key words: defense chemistry; diarylheptanoids; ecosystem subsidies; ellagitannins; indirect effects; intraspecific variation; local adaptation; trophic interactions.

Introduction

Organisms are tightly interconnected in tangled webs of interactions. Variation in organismal diversity across space and time can have cascading effects across multiple trophic levels (Bruno and O'Connor 2005), and even across-ecosystem boundaries. There are many examples of the tight interconnection between terrestrial and aquatic systems, particularly forest-river systems (Nakano and Murakami 2001, Knight et al. 2005). Preservation of biodiversity is a well-accepted means of preserving many key ecosystem functions by maintaining ecosystem resistance and resilience to disturbance (Cardinale et al. 2006, Ives and Carpenter 2007), but the mechanisms explaining why diversity maintains ecosystem stability are less known (Ives and Carpenter 2007). Understanding the effects diversity may have on adjacent ecosystems is critical for predicting and mitigating consequences of declining diversity. Species diversity remains the focus of biodiversity studies, but recent work has expanded this field into how biodiversity at the within-species scale affects community structure and ecosystem processes (Crutsinger et al. 2006, Whitham et al. 2006). Studying intraspecific diversity also illuminates the development of linkages at temporal and geographic scales, and points to possible experiments in nature.

Our study examines how selective forces driving divergence and creating diversity ultimately affect adjacent ecosystems receiving subsidies. For example, a major component of plant diversity often arises from plastic and genetic responses to herbivore stress. Plant defenses against herbivores are varied and include production of mechanical and chemical defenses, reduction in tissue quality, and volatile signals to attract predators of the herbivores to sources of infestation (Agrawal 1998, Allmann and Baldwin 2010). Defenses employed by plants often depend on the availability of environmental resources and genetics. Neighboring individuals may share common abiotic resources such as nutrients, have closer genetic relatedness, and experience similar biotic pressures such as herbivory than individuals growing a distance apart (Coley et al. 1985, Schweitzer et al. 2008). Together, these spatial factors can cause a geographic mosaic of interactions (Thompson 2005) resulting in sustained spatial variation in plant diversity with potential consequences for other dependent organisms, such as the terrestrial and aquatic decomposers that consume 80–90% of carbon fixed by plants (Cebrian 1999). Assuming then that consumers should benefit from being adapted to efficiently consume available resources, in a scenario where we see spatial structuring in leaf traits of a plant species (such as defensive chemistry), do communities of consumers in recipient systems vary to efficiently match the plants in adjacent donor communities with different chemical signatures?

We address this question using riparian red alder trees (*Alnus rubra*), a dominant deciduous tree in the Pacific Northwest, as the model system where intraspecific variation in leaves has strong effects on herbivory rates, decomposition in soils, and decomposition in streams

Manuscript received 5 October 2015; revised 11 January 2016; accepted 28 January 2016; final version received 14 March 2016. Corresponding Editor: J. B. Yavitt.

[1] E-mail: sjackrel@uchicago.edu

(Jackrel and Wootton 2014, 2015). Previously, we showed that induced defense responses of red alder trees to terrestrial herbivory stress slow leaf decomposition in streams (Jackrel and Wootton 2015). Additionally, intraspecific variation in red alder leaves causes local matching that enhances rates of aquatic and terrestrial ecosystem function at small scales (<1.0 km) (Jackrel and Wootton 2014, 2015). We used reciprocal transplant experiments to show that local communities decomposed leaves from red alder trees growing in the immediate area more quickly than leaves from trees growing at further distances. These opportune systems with trophic effects crossing the aquatic-terrestrial boundary enable us to study the implications of intraspecific diversity on aquatic decomposers largely decoupled from the terrestrial herbivory processes shaping spatial patterns of diversity among trees. Leaf decomposition results from complex interactions among invertebrates, microbes, and hyphomycetes (Wright and Covich 2005). In this study, we demonstrate a chemical basis for the significant ecological variation we observed.

Here, we document presence and relative abundance differences in 10 diarylheptanoids (including two with mass spectra consistent with novel structures) and 13 ellagitannins in leaves from a population of 40 red alder trees growing along the banks of four rivers. Diarylheptanoids are notable in the biomedical literature for their toxicity (Sati et al. 2011) and promise for cancer treatments (Farrand et al. 2014); some evidence also suggests diarylheptanoids inhibit digestion in herbivores (Sunnerheim and Bratt 2004). We took advantage of technical developments to characterize these compounds and explore their ecological importance (González-Hernández et al. 2000, Muilenburg et al. 2011). Recent reviews stress that ellagitannins are an underappreciated class of secondary metabolites (Salminen and Karonen 2011), and plants are known to suppress ellagitannin production in response to reduced insect pressures (Agrawal et al. 2012). Ellagitannins may function as an herbivory defense via their oxidation activity, which can damage nutritional quality (Barbehenn et al. 2006). Because the relative magnitude of oxidation activity in ellagitannins differs from other tannins, which are less easily oxidized but rather are much more effective at binding and inhibiting digestion of plant proteins, traditional functional metrics (such as assays measuring protein-precipitation capacity) that are still frequently used for measuring secondary metabolites are inadequate to fully characterize plant defensive compounds (Stevens et al. 2014, Mason et al. 2015). We use high-resolution (i.e., accurate mass) mass spectrometry that enabled precise separation within classes of compounds (e.g., different ellagitannins) and allowed us to characterize specific compounds that may play important roles in ecology and ecosystem function. Here, we show how secondary metabolites, nutrients, and mechanical defense vary in a natural population of trees and regulate local stream decomposition rates. Further, our results show that aquatic and terrestrial decomposer communities are locally matched to leaf defensive chemistry differences in the local red alder individuals that frequently supply abundant leaf litter to these communities.

Materials and Methods

To determine the driving factor behind local adaptation to intraspecific plant variation in decomposer communities, we first measure intraspecific leaf and tree traits: including secondary metabolites (ellagitannins and diarylheptanoids), nutrients (C, N, and P and the isotopes of C and N), leaf thickness, and trunk diameter. We ask which traits best predict aquatic ecosystem function using data from leaf pack experiments. After finding that ellagitannins are one of the strongest predictors of aquatic decomposition, we use the structure of each ellagitannin to predict the strength of their function (oxidation) against consumers. We then determine whether strength of oxidative function is predictive of aquatic decomposition. Next, we test whether secondary metabolite composition can be predicted by other leaf traits, and whether these metabolites vary geographically. After finding geographic structuring, we completed a diet field experiment to determine whether this geographic variation in chemical components drives adaptation in streams and soils.

Study sites

Red alder is an abundant deciduous tree in riparian zones of the Pacific Northwest. We chose 40 trees growing along four rivers in the Olympic Peninsula of Washington State: the South Fork Pysht (48.167° N, 124.157° W), Hoko (48.261° N, 124.354° W), Little Hoko (48.255° N, 124.343° W), and Sekiu (48.282° N, 124.409° W) (for river descriptions, see Jackrel and Wootton 2014). Riparian zones at each river consisted of early successional forest dominated by red alder with small numbers of bigleaf maple (*Acer macrophyllum*), western hemlock (*Tsuga heterophylla*) and other conifers.

Leaf field experiment and leaf preparation

To test how individual variation in alder leaf traits affects aquatic ecosystem function, we used data on leaf decomposition rates in streams from our previous experiment (Jackrel and Wootton 2014). This experiment was replicated in two different pairs of similar sized rivers (between two fourth-order streams, Sekiu River and Hoko River, and between two third-order streams, South Fork Pysht River and Little Hoko River). In brief, green leaves were collected from five red alder trees growing in the riparian zone immediately upstream of each of the eight aquatic deployment sites (two sites per river and 40 trees in total) and used to construct four leaf packs per tree to measure decomposition rate at four locations: two sites in the adjacent river and two sites in the paired river

(see Appendix S3 for an illustration of the reciprocal transplant experimental design). Green leaves are a substantial and consistent energy resource available in these streams for aquatic decomposers during their summer growing season, a time when high quality resources are essential (Stout et al. 1985, Jackrel and Wootton 2014). Initial and final leaf weights were recorded for each leaf pack, yielding four decomposition rates per tree. These data were collected from the Pysht and Little Hoko rivers in July 2012 and the Hoko and Sekiu Rivers in August 2012 (Jackrel and Wootton 2014). Our linear mixed-effects models use individual tree identity as our random effect for our four repeated decomposition measurements, and due to the experimental design, tree identity also incorporates temporal differences between the two experimental rounds.

As an indicator of leaf thickness, we took leaf cores 12 mm in diameter from an additional 20 leaves per tree, then oven dried for 48 h and weighed each core to the nearest milligram. As a proxy for tree age, we measured tree trunk diameter at 1.5 m above ground. Additional leaves were oven dried, ground in a mortar, and stored at room temperature until further analyses.

CNP measurements

We packed 3 mg of leaf powder into 3.5 × 5 mm tin capsules and measured percent nitrogen, percent carbon, and $^{15}N/^{14}N$ and $^{13}C/^{12}C$ ratios using a Costech 4010 Elemental Analyzer combustion system coupled to a Thermo DeltaV Plus IRMS via a Thermo Conflo IV interface at the University of Chicago Stable Isotope Ratio facility. The reproducibility was 0.11‰ for ^{13}C and 0.17‰ for ^{15}N, and cocoa powder and glutamic acid were used as isotopic controls. To measure phosphorus we used an ashing, acid-hydrolysis, and phosphomolybdate-blue spectrophotometric protocol (Jackrel and Wootton 2015). In addition to %C and %N, total C and N isotopic ratios were measured as proxy indicators for different leaf components (e.g., ^{13}C-depleted leaves may contain more lignin, while ^{13}C-rich may contain more polysaccharides [Benner et al. 1987, Teece and Fogel 2007]).

Mass spectrometry analyses

We extracted 100 mg of leaf powder in 10 mL 70% methanol at ambient temperature, and auto injected 5 μL aliquots of each sample through a Zorbax SB-C18 2.1 × 150 mm, 3.5 μm column on an Agilent Q-TOF LC-MS with dual ESI (Agilent 6,520). We ran each sample separately in negative mode and positive mode using the Auto MS/MS mode with the following parameters: 35 eV fixed collision energy, 325°C gas temperature, 9 mL/min drying gas, 40 psig nebulizer, 170 V fragmentor, 120 V skimmer voltage, 750 V OCT 1 RF Vpp, and 4,500 V capillary voltage. We eluted the samples with 0.1% formic acid in water (A) and 0.1% formic acid in 100% methanol (B). The separation was carried out with the following program: 5 min of 100% A at a rate of 0.2 mL/min, followed by a gradient from 100% to 60% A (0% to 40% B) over 20 min at a rate of 0.1 mL/min. Flow was then held for 5 min at 60% A (40% B) at a rate of 0.3 mL/min. Then a gradient from 60% to 0% A (40% to 100% B) was carried out over 15 min at 0.3 mL/min, and then held for 10 min at 0% A (100% B) at 0.3 mL/min. Additionally, we did targeted Q-TOF runs in High Resolution mode at varied collision energies in precursor and product ion modes to further aid compound characterization (data not shown).

We characterized compounds using retention times and fragmentation patterns of chromatograms with automatic agile integration using Agilent Mass Hunter Software (Qualitative Analysis B6 2012). Additional software was used for heuristic filtering of the obtained molecular formulas (Kind and Fiehn 2007). Commercial standards including oregonin (Sigma-Aldrich, CAS #55303-93-0) and curcumin (Sigma-Aldrich, CAS #458-37-7, St. Louis, Missouri, USA) were used to aid in characterization. We recorded base peak chromatogram (BPC) abundance for each peak, standardized abundance as BPC per milligram of leaf material extracted to account for slight deviations from 100 mg of leaf powder extractions, and log transformed BPC data to consider relative compound abundances. Samples from all forty trees were run on the machine in a randomized order to control for any potential deviations over time in mass spectrometer performance.

Diet field experiment

In a second field experiment, we measured potential responses to individual variation in leaf chemistry by offering to decomposers extracted leaf compounds in an agar matrix. We completed these experiments using the same river pairings as in previous reciprocal transplant experiments (see Appendix S3 for an illustration of the experiment). We collected leaves from the 40 alder trees in June 2013 and used the same protocol for extracting secondary metabolites as described for mass spectrometry analyses. We allowed the methanol fractions to evaporate and then resuspended the remaining residue in 10 mL of water. We prepared a general purpose Lepidoptera diet (BioServe, Product #F9772, Flemington, New Jersey, USA) according to package instructions except for doubling the gelling agent to avoid disintegration of the diet underwater (10.5% supplied agar, 10.5% agarose (Sigma-Aldrich), and 79% dry diet). We chose this proportion of agar, agarose, diet, and water because we found this formula resulted in no visible fragmentation or substantial mass loss after submerging in tap water for 7 d. We added 10 g of prepared diet into glass vials, warmed the vials to melt, added 3.3 mL of tree-specific extract, and mixed thoroughly. We immediately loaded liquid diets using 10 cc syringes into randomly selected well locations in 96-well microplates in

batches of four plates (e.g., one plate for each of four sites in the Pysht and Little Hoko Rivers). Each of these plates contained 20 different types of diets, one for each of the 20 trees growing along one set of the paired rivers.

For aquatic plates, we surrounded diet options by empty wells and used the middle of each plate to avoid edge effects. We repeated the experiment twice for a total of 16 plates across four rivers. We recorded starting mass of each well filled with diet by taring the balance between diet additions. We placed each plate in bags made of 4.75 mm mesh nylon seine netting fixed across the plate surface with mini-binder clips. This arrangement permitted feeding while proving a gripping surface for macroinvertebrates, and enabled attachment to the stream bed via cable ties attached to steel reinforcing bars pounded into the stream bed (Appendix S3). We secured plates to the stream bed immediately downstream of the five study trees at each deployment site along the four rivers. We retrieved plates after 2–6 d, depending on general feeding rate, with the goal of removing plates once ≈ 50% of the diet had been consumed. We weighed each well of diet to the nearest centigram and calculated percent mass lost. We observed caddisflies, which are known to consume alder litter, actively feeding on the diets. However, we note that in situ feeding experiments cannot preclude other consumers that may not typically feed on intact leaf litter (such as algivores). Any mass loss due to algivore feeding or abiotic processes was controlled by our randomized intermixing of home and away diets that minimized any systematic differences in biotic and abiotic conditions affecting each group.

In riparian soil, instead of duplicate rounds, we assigned each specific diet to two well locations per plate, filling the top four rows of cells. We filled each well to the rim, but did not measure starting weights. The average starting weight for each individual well of diet from the 16 aquatic plates ($\mu = 0.420$ g $\pm$ 0.0089 SD) was substituted as the approximate starting weight of each well of diet for the soil plates. We placed plates in mesh bags, secured with mini-binder clips, and buried the plates beneath 10–15 cm of soil under the most downstream tree at each deployment site along the Pysht and Little Hoko rivers. We did not implement the experiment in the Sekiu and Hoko rivers. Plates were retrieved after 29 d, washed gently to dislodge soil, weighed to the nearest centigram, and percent mass loss for each well was calculated. Replicate measures were incorporated into a nested random term of analysis of variance models, as described in detail below.

Statistical analyses

We describe variation in 35 chemical compounds among 40 trees using a principal component analysis. Principal components were extracted using singular value decomposition of the correlation matrix to weight common and less common compounds equally (prcomp function, R Development Core Team, 2014). We tested whether ellagitannin content (via PC1 scores), diarylheptanoid content (via PC2 scores), and flavonoid content (via PC3 scores) were predicted by measured tree traits (including leaf %C, %N, %P, leaf thickness, and trunk diameter) using linear regression (Table S2D). We tested what traits (including leaf %C, %N, %P, leaf thickness, trunk diameter, and scores for PC1, 2 and 3) best predicted decomposition rates in rivers using linear mixed-effects models with individual tree as the random effect. In addition to using PC scores as metrics of secondary metabolites, we also tested which specific compounds (either within the class of ellagitannins, or within diarylheptanoids) best predicted decomposition rates in rivers using linear mixed-effects models. We selected best fitting models by comparing AIC scores and for mixed-effect models report marginal R^2 values to describe variance explained by the fixed factors (Nakagawa and Schielzeth 2013). We tested whether differences in chemical classes (quantified as differences in scores along each principal component) among trees corresponded to geographic distance among trees using a Mantel test. Because ellagitannins can be quite complex in molecular structure (Karonen et al. 2010) and vary six-fold in their oxidative capacity, we estimated oxidative function of each ellagitannin using the following formula (Barbehenn et al. 2006, Moilanen and Salminen 2008):

$$\mathrm{OA} = (15.5A + 6.6B + 4.9C + 4.5D + 3.6E + 1.9F + 1.1G)/W$$

where A = number of valoneoyl groups, B = number of nonahydroxytriphenoyl groups, C = number of valoneoyl or sanguirsorboyl groups, D = number of xylose/lyxose groups, E = number of acyclic castalagin-type glucoses, F = number of hexahydroxydiphenoyl groups, and G = number acyclic vescalagin-type glucoses, and W is the molecular weight of the ellagitannin (g/mol). We then used these calculations to ask whether the ellagitannins selected by our model as the strongest predictors of decomposition in rivers also had relatively strong oxidative function.

For the diet experiments, we tested whether diets prepared from alder leaves sourced from different relative locations decomposed at different rates using a five group ANOVA. The diets were prepared from trees either growing (1) at the home site on the home river; (2) upstream on the home river; (3) downstream on the home river; (4) upstream on the away river; (5) or downstream on the away river. Our two fixed factors were this home/away variable and tree identity, and our two random factors were deployment location and a nested term of plate replicate nested within tree identity and deployment location. Because we had hypotheses based on prior results from reciprocal transplant leaf pack experiments in streams (Jackrel and Wootton 2014), we used our a priori ordered predictions to calculate a directional five-group ANOVA using Spearman rank correlations (Rice and Gaines 1994). For the riparian soil data, we used a

three-group ANOVA (home site, away site on the home river, or away river) because we did not have an a priori expectation that upstream vs. downstream sites on the home river would yield different results in a terrestrial system.

To test whether alder trees growing in geographic proximity were more similar in chemical composition than distant neighbors, we constructed a chromatogram distance matrix among trees (with elements S_{ij}) by calculating pairwise Euclidean distances between tree pairs:

$$S_{ij} = \sqrt{\sum_{k=1}^{35} (C_{ik} - C_{jk})^2}$$

where C_{ij} is the log BPC of chemical compound k in tree i. We log transformed data because relative ratios of chemical compounds are often essential for conferring information (Christensen et al. 1989). We tested whether this chromatogram distance matrix was significantly correlated with a geographic distance matrix (using GPS coordinates for each tree) using a Mantel test. We determined whether a model including chromatogram data alone could predict tree growing location in nature with a discriminant function analysis (DFA) (SPSS IBM Corp. 2013, Armonk, New York, USA). Using the DFA, we identify which chemical compounds differ most among riparian sites. To maximize statistical power and identify a more parsimonious model, we entered all 35 chemical compounds into the model and iteratively removed variables one-by-one by selecting the variable with the smallest standardized coefficient on DF1 until any additional removal reduced cross-validation reclassification accuracy. We report these results with and without leave-one-out cross-validation, because our experimental design required an unusually large removal (20%) of the original data set one of the five trees per riparian site).

Results

Each red alder tree contained a mixture of 35 compounds that were eluted within the first 45 min of each chromatography column run (Fig. 1). We characterized 13 ellagitannins (Appendix S1: Fig. S1), three flavonoids, and 10 diarylheptanoids (Appendix S1: Fig. S2) (Appendix S1: Table S1 provides references for each characterization). Ellagitannin elution order has been clearly modeled (Moilanen et al. 2013), which facilitates mass spectrometry characterization. We characterized each compound, molecular mass, and formulae of parent molecules, fragmentation patterns, and corresponding peak numbers, as illustrated (Fig. 1). The ellagitannin di-HHDP-glucose (consistent with pedunculagin α), diarylheptanoid oregonin, and flavonoid quercetin glucuronide were generally observed at the highest levels in each tree chromatogram (Appendix S1: Table S1). We found two potentially novel diarylheptanoids with mass spectra not yet reported in the literature, and though definitive identification will require future investigations via NMR, both contain glucose rather than xylose and elute prior to previously studied compounds, as expected given the increased polarity of the glucoside (Appendix S1: Fig. S2, Table S1).

Principal components analysis independently separated the chemical signatures of individual trees primarily along the three compound families (ellagitannins, diarylheptanoids, and flavonoids; Appendix S4: Table S1; Fig. 2). The first axis is loaded most strongly by nine ellagitannins, the second axis is loaded with eight diarylheptanoids, and the third axis contains the three

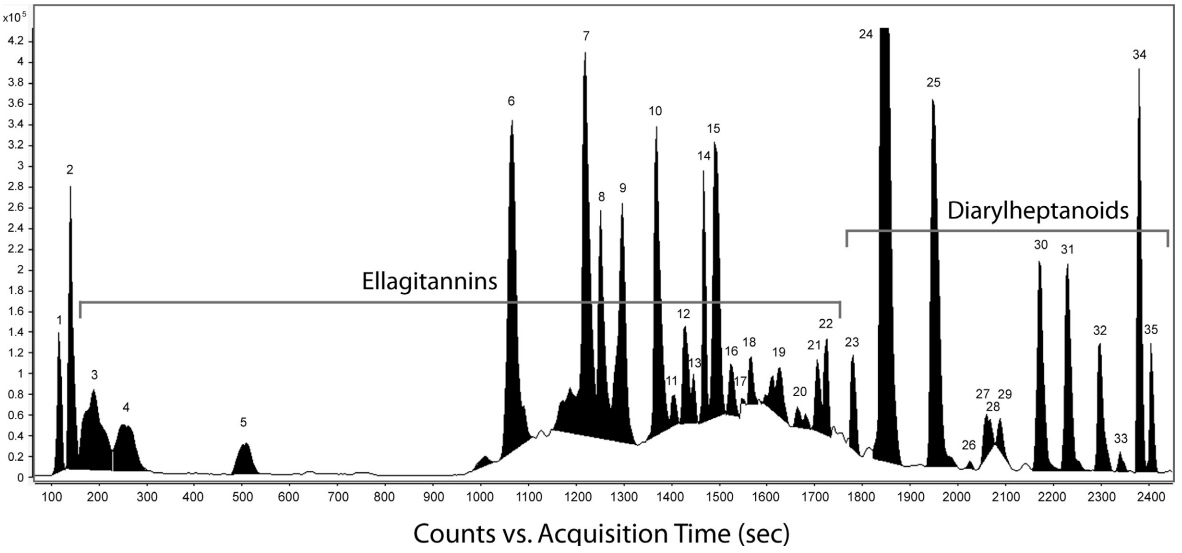

Fig. 1. Example chromatogram from a red alder tree growing in the riparian zone of the Pysht River (ELK 4). Black shading indicates the area of each peak after baseline correction. Note peak 24 (oregonin) is cutoff to provide a better view of less relatively abundant compounds.

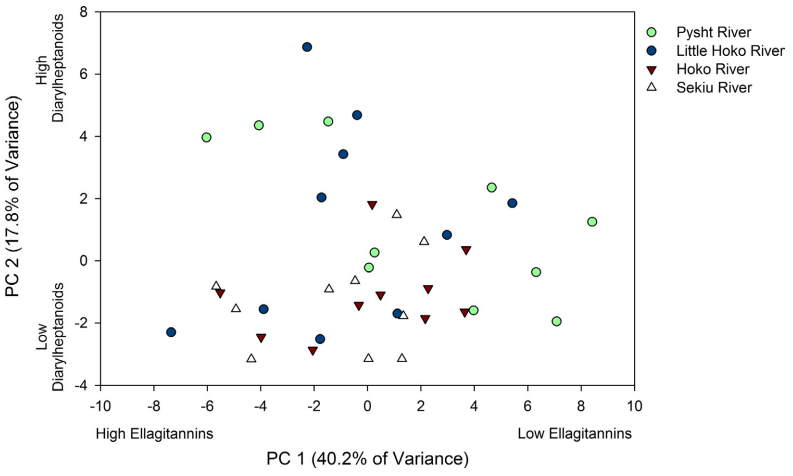

FIG. 2. Individual red alder trees growing in the riparian zones of four rivers vary in leaf chemistry along a largely ellagitannin axis and of secondary importance, a diarylheptanoid axis via a principle component analysis. The analysis includes 35 variables, one for the size of each of the 35 peaks as shown in Fig. 1. See Appendix S4: Table S1 for PC loadings.

flavonoids (Appendix S4: Table S1). Trees varied considerably in secondary metabolite composition: some ellagitannin relative abundances varied over 12-fold (#15 di-HHDP-galloyl-glucose β, consistent with casuarictin) and some diarylheptanoids varied over 300-fold (#23 HOG). We then asked if this variation in defensive compounds corresponded with ecologically important traits, most of which showed substantial variation within the population: %N content ranged two-fold (mean 2.89% ± 0.42% SD), %P content ranged three-fold (0.16% ± 0.047%), leaf thickness ranged four-fold (0.007 ± 0.002 g/unit area^2), tree diameter ranged 46-fold (55.8 ± 24.1 cm), and $^{15}N/^{14}N$ ranged three-fold (−1.48‰ ± 0.27‰), whereas $^{13}C/^{12}C$ was fairly constant (−32.00‰ ± 0.97‰). Stepwise regression showed that trees with leaves containing a high relative abundance of ellagitannins, as measured by PC 1, tended to contain less nitrogen and relatively less phosphorus (i.e. elevated N:P) ($F_{2,37}$ = 13.84, P < 0.001; Appendix S2: Table S1, Appendix S4: Table S1; Fig. 3a). Trees with leaves containing high relative abundances of diarylheptanoids, as measured by PC 2, tended to have thinner leaves, reduced C:P and elevated C:N and N:P than leaves lower in diarylheptanoids ($F_{4,35}$ = 10.42, P < 0.001; Appendix S4: Table S1, Appendix S2: Table S2). Leaf flavonoids (PC 3) exhibited a weak inverse correlation with $^{15}N/^{14}N$ (Appendix S2: Table S3).

We then found that leaf decomposition in streams is best predicted by both chemistry and mechanical traits. Based on our leaf pack experiments across four rivers, ellagitannin content (as represented by PC1) and leaf thickness were the best predictors of leaf decomposition rate in streams (marginal R^2 = 0.48, n = 148 leaf packs; Appendix S2: Table S4), exceeding all other measured variables including all of our nutrient variables, tree diameter, diarylheptanoid content (as represented by PC2), and flavonoid content (as represented by PC3). Ellagitannin content alone explained 18% of the variance in decomposition rate (Fig. 3b), and we found that disparity among pairs of red alder trees along this ellagitannin axis (via pairwise distances between PC1 scores) corresponded with geographic distance between them (Mantel test, P = 0.014). Among the 13 compounds largely contributing to that ellagitannin axis of PC1 (Appendix S4: Table S1), HHDP-galloyl-glucose (consistent with isostrictinin) and di-HHDP-galloyl-glucose β (consistent with casuarictin) appeared to be the strongest inhibitors of aquatic decomposition (linear mixed-effects model: marginal R^2 = 0.30, HHDP-galloyl-glucose, t_{37} = 3.0, P = 0.0048, di-HHDP-galloyl-glucose β, t_{37} = −4.7, P < 0.001). When we used molecular structure to calculate approximate oxidation rate for ellagitannins we characterized in red alder, these two compounds had among the highest oxidation rates (4.1 and 4.9 abs/s/mM; Appendix S1: Table S1).

Relative abundance of several diarylheptanoids also predicted substantial variation in aquatic decomposition rate (linear mixed-effects model: marginal R^2 = 0.155, methylhirsutanonol t_{35} = 2.11, P = 0.043, oregonin t_{35} = −1.73, P = 0.093, platyphylanolanol-xyloside t_{35} = −2.10, P = 0.043, alnuside A t_{35} = 1.77, P = 0.086). Additionally, these compounds were fairly variable in the population (mean relative abundance ±1 SD of each compound is reported in Appendix S1: Table S1), but unlike ellagitannins, this variation did not correspond with the scale of geographic distances our study explored: pairwise distances between PC2 scores were not correlated with geographic distance between red alder trees (Mantel test, P = 0.15).

We constructed a chromatogram distance matrix to consider the relative abundances of all 35 chemical compounds, and we again found that red alder trees growing in geographic proximity shared more similar secondary metabolite chemistry than more distant neighbors

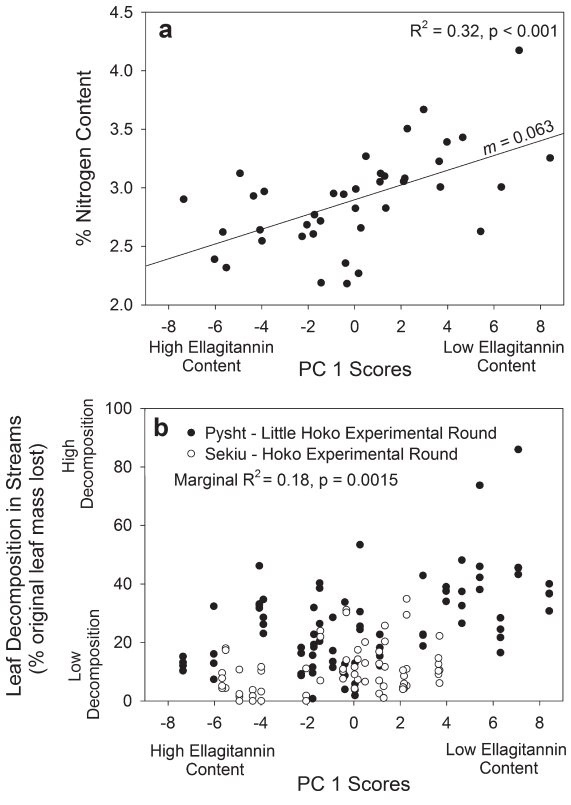

FIG. 3. Variation in ellagitannins (as shown by PC 1 of Appendix S4: Table S1) predicts (a) % nitrogen content of leaves from individual red alder trees and (b) aquatic decomposition rate of leaves in streams.

(Mantel test, $P = 0.0035$). Entering all 35 compounds in a discriminant function, across the eight riparian sites (Wilk's $\lambda < 0.001$, $\chi^2_{189} = 288.9$, $P < 0.0001$), illustrates the strong effects of geography on the chemical profiles of these trees. The first discriminant function accounted for 93.9% of the variation and was such a strong predictor of geographic location that 100% of the 40 trees were classified to the correct site on the correct river (compared to 12.5% correct classification by chance) (Fig. 4). Even when removing 20% of the original data to enable cross-validation, reclassification was correct in 45% of the trees, which is 3.5-fold more trees than expected by chance. The first discriminant function is a complex compilation of 27 compounds (Appendix S5: Table S1), including at least 13 ellagitannins, which as we showed above are generally strong predictors of aquatic decomposition.

We found that this spatial structuring of ellagitannins, diarylheptanoids, and flavonoids in riparian trees drove local decomposer responses both in the terrestrial and riparian environment. To separate chemistry from structural leaf properties, we prepared 40 diets containing tree extracts (prepared in the same way as extracts loaded onto the mass spectrometer) for in situ feeding experiments. We found aquatic communities consumed diets prepared with local red alder extracts 24.7% more than diets prepared with red alder growing along a different river. We also found this same pattern of local matching at the within-river scale. Our a priori prediction was that communities are most efficient at consuming chemical components that are present in leaves supplied to that particular location. Due to our experimental design, our away sites on the home river represent one of two scenarios: at downstream sites, leaves from the upstream site wash downstream and represent a natural food resource, but at upstream sites, leaves from the downstream sites wash further downstream and represent a novel food resource. In the first scenario, we found that aquatic communities consumed 11.2% less diet prepared from alder trees growing at an upstream site on the same river compared to trees growing at that deployment site, but in the second scenario, aquatic communities consumed 19.9% less diet prepared from alder trees growing at a downstream site on the same river (Fig. 5a, Table 1; $P < 0.025$, ordered heterogeneity test). This result emphasizes that regular exposure, rather than distance alone, appears to

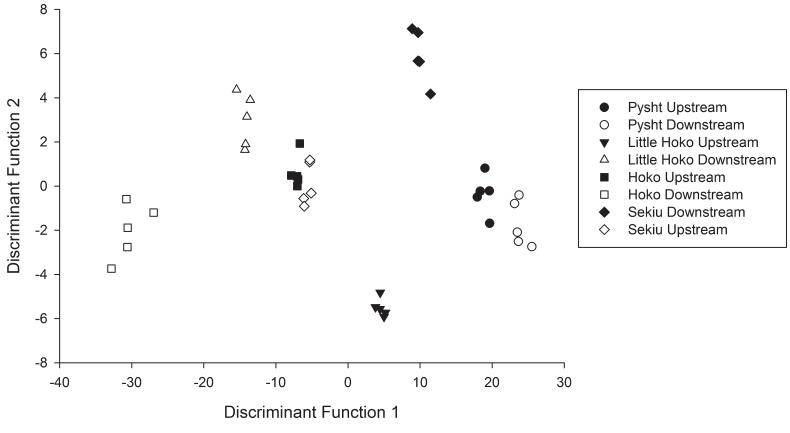

FIG. 4. Secondary metabolite composition of 40 riparian alder trees groups trees into actual growing locations in nature via discriminant function analysis.

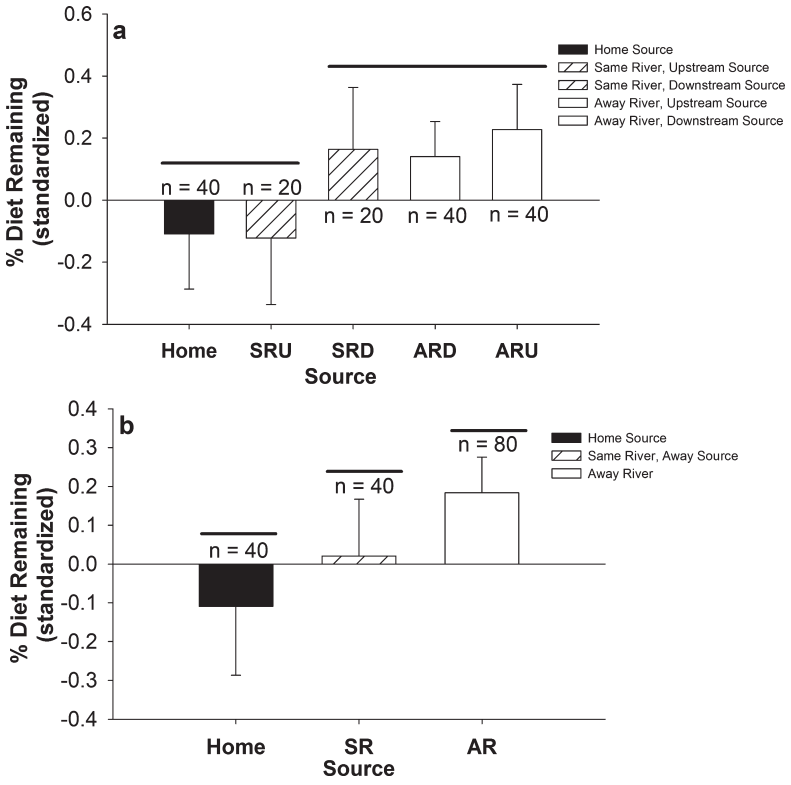

FIG. 5. Average decomposition (±SE) in (a) streams and (b) soils of forty commercial diets prepared containing added leaf extracts from individual red alder trees.

TABLE 1. Analysis of variance comparing aquatic decomposition rates of diets containing red alder leaf extracts from individual riparian trees that were each deployed at four sites: the home site immediately downstream of the focal tree, the same river at a different site either upstream or downstream of the focal tree, and at two sites on a different river.

Source	df	SS	MS	*F*	*P*‡
Leaf source	4	0.056	0.014	1.371	
Home river vs. away river	1	0.032	0.032	3.171	<0.025
Local vs. non-local†	1	0.051	0.051	5.100	<0.025
Tree identity	38	0.539	0.014	1.382	
Error	160	6.99	0.044		

Notes: Indented lines are planned a priori comparisons. †Local indicates diets made using extracts from red alder trees growing at the deployment site (Home in Fig. 5a) or a same river site upstream (SRU in Fig. 5a). Non-local indicates diets were made using extracts from trees growing downstream of the deployment site, or a different river entirely (indicated SRD, ARD, ARU in Fig. 5a). ‡Reported *P*-values include a-priori ordered heterogeneity corrections (Rice and Gaines 1994).

contribute to local adaptation. We regularly observed *Psychoglypha* and *Dicosmoecus* caddisflies feeding on aquatic plates and assume them to be important consumers.

We found a similar pattern of local adaptation in riparian soils: the soil community consumed diets prepared from local red alder diets 11.3% more than diets prepared from red alder growing elsewhere along the same river, and 25.4% more than diets prepared from red alder growing next to different rivers (Fig. 5b; $P < 0.025$, ordered heterogeneity test).

DISCUSSION

Variation in food resource quality affects consumer movement patterns, metamorphic and reproductive decisions, and plastic and genetic changes in physiology (Hunter and McNeil 1997, Awmack and Leather 2002). We show that variation within species in one ecosystem can alter key processes in another ecosystem through fluxes across boundaries. By pairing mass spectrometry data with reciprocal transplant experiments in the field, we show that intraspecific variation in plant chemistry drives an ecosystem function in streams and causes local terrestrial and aquatic communities to adjust to local leaf chemistry. Geographic variation among complex mixtures of secondary metabolites, notably ellagitannins, seems to drive these local matching patterns, which are evident at large (across-river) and small (within-river) scales. Within rivers, diets containing secondary metabolite extracts from upstream trees decompose quickly at

downstream locations relative to diets from downstream trees at upstream locations, further suggesting that it is the exposure to leaves from local trees that is driving this process among aquatic decomposer communities. These results demonstrate that terrestrial processes shaping the chemical composition of ecosystem subsidies from donor habitats drives locally adaptive changes in recipient communities.

Red alder trees were highly variable in two classes of secondary metabolites: ellagitannins and diarylheptanoids. Both classes of compounds have only just begun to receive ecological consideration (Salminen and Karonen 2011), primarily for technical reasons. We show how frequent drivers of consumer population ecology, such as leaf nutrients and thickness, are correlated with these secondary metabolites. Further, we show that ellagitannin variation plays a key role in affecting rates of decomposition in streams. To estimate tannin content, studies have used functional metrics to measure important anti-herbivory properties, such as protein-precipitation capacity. Condensed tannin content correlates well with this measurement, but ellagitannins are poor protein precipitators and are consequently underestimated in these assays, and more generally have been underestimated in their ecological importance. Ellagitannins, however, are strong oxidants, a chemical property associated with increased metabolic costs in alkaline guts of herbivores, such as those of terrestrial lepidopterans and aquatic Chironomidae and Tipulidae insects (Clark 1999, Barbehenn et al. 2009, Salminen and Karonen 2011). Our finding that aquatic decomposition was best estimated by relative abundances of ellagitannins with relatively high oxidative measures, suggests that oxidative function may be important in aquatic systems. Therefore, we need additional studies that consider the role of ellagitannins in plant defense, insect metabolism, and decomposition by microbes and hyphomycetes.

Diarylheptanoids are found in substantial diversity in alder species (Sati et al. 2011), including at least six in the bark of red alder (González-Laredo et al. 1998, Chen et al. 2000). Our results show they are present in leaves, and are thus of relevance to folivores. Ecological studies on diarylheptanoids are limited, but biomedical research (Farrand et al. 2014) and traditional medicine records (McCutcheon et al. 1994) have noted anti-microbial and anti-oxidant properties, suggesting these compounds likely play substantial ecological roles. Interestingly, given their noted toxicity, we found that several diarylheptanoids appear to inhibit decomposition. However, given their limited geographic variation at the scales we studied, they seem unlikely to explain the local adaptation patterns of decomposition in this system.

In our previous work, we have shown that induced plant defense to herbivory stress suppressed detrital energy capture in streams (Jackrel and Wootton 2015). We found that red alder trees given an herbivory stress showed a marked decline in leaf nitrogen content, and thus aquatic decomposers preference for nitrogen-rich leaves seemed to be driving the observed effect on aquatic ecosystem function. Here, in a nonexperimental setting, we found that ellagitannins are a stronger predictor of aquatic decomposition than %N (Appendix S2: Table S4), but there is a negative correlation between ellagitannin and nitrogen content ($R^2 = 0.32$). Soil nitrogen additions are not known to effect ellagitannin content (estimated as ellagic acid equivalents) in non-nitrogen fixing trees including poplar, maple and oak (Kinney et al. 1997), but condensed tannins from poplar can inhibit nitrogen fixation in thinleaf alder (Schimel et al. 1998). Further study may clarify the interactive effects among induced defense responses to herbivory, ellagitannin production, and nitrogen fixation and allocation.

We found ellagitannin, diarylheptanoid and flavonoid variation were all correlated with leaf traits, such as thickness and nutrients that are well-known to affect consumers (Coley 1980, Mattson 1980, Jackrel and Wootton 2015). But our results from both leaf pack and diet experiments suggest ellagitannin content is a greater predictor of ecosystem processes than nutrients (Appendix S2: Table S4), and therefore warrants further study into plant production pathways of these compounds and the ecological implications of relative nutrient vs. defense compound content in red alder and other plants.

The importance of intraspecific diversity has only recently been recognized in a community ecology context (Violle et al. 2012). We show that spatially variable factors such as genetics, environmental resources, or ecological interactions caused tree conspecifics growing a distance apart to produce more divergent leaf chemistry traits than nearby neighbors. Different genetic constraints may lead to variation in chemistry under similar environmental pressures, as in the genetically controlled variation of condensed tannins in cottonwoods (Schweitzer et al. 2004). Alternatively, divergent chemistry could be caused by environmental gradients in soil nutrients or variation in plant-insect interactions due to spatial changes in terrestrial herbivore composition or densities (Bryant et al. 1987, Lankau 2007). Determining the relative contributions of and interaction between genetic and environmental factors in spatial variation of plant subsidies is an important future direction for predicting how natural and anthropogenic changes to the terrestrial environment will affect stream systems.

To predict the extent of such interactions in nature, we need to investigate the evolutionary development of these complex cross-ecosystem interactions. To do this, we need to understand the mechanisms of aquatic and terrestrial decomposers matching to these local subsidies. Accelerated decomposition efficiency may be arising from shifts in community composition (such as shifting aquatic invertebrates along gradients in stream size [Vannote et al. 1980]) or phenotypically plastic or genetic shifts in individuals. Comparing stream and riparian decomposer communities in this system provides an ideal opportunity to compare evolutionary trajectories to local

adaptation in the presence and absence of feedback interactions of decomposition processes on host trees. These insights may suggest the time-scale needed for these processes to occur, and therefore their potential generality in other ecosystems.

Acknowledgments

We thank J. Bergelson, G. Dwyer, C. A. Pfister, and T. D. Price for constructive comments and discussion on this work. This work was supported by the NSF GRFP, the DOE GAANN, NSF DDIG DEB-1311293, ARCS (Achievement Rewards for College Scientists) Foundation, Inc.'s Scholar Illinois Chapter (2014 and 2015), and University of Chicago Hinds Fund grants to SLJ; an Olympic Natural Resources Grant and NSF grant DEB 09-19420 to JTW; and NSF grant OCE-0928232 to C. A. Pfister. We thank A. Colman, A. Mine, G. Olack and the Colman Isotope Lab at University of Chicago for assistance with nitrogen, carbon and phosphorus analyses. We thank Merrill & Ring Inc., J. Murray, M. Hurd, D. Hurd, Hoko River State Park, and the Washington State Department of Natural Resources for providing facilities and facilitating research on their lands.

Literature Cited

Agrawal, A. A. 1998. Induced responses to herbivory and increased plant performance. Science 279:1201–1202.

Agrawal, A. A., A. P. Hastings, M. T. J. Johnson, J. L. Maron, and J.-P. Salminen. 2012. Insect herbivores drive real-time ecological and evolutionary change in plant populations. Science 338:113–116.

Allmann, S., and I. T. Baldwin. 2010. Insects betray themselves in nature to predators by rapid isomerization of green leaf volatiles. Science 329:1075–1078.

Awmack, C. S., and S. R. Leather. 2002. Host plant quality and fecundity in herbivorous insects. Annual Review of Entomology 47:817–844.

Barbehenn, R., C. Jones, A. Hagerman, M. Karonen, and J.-P. Salminen. 2006. Ellagitannins have greater oxidative activities than condensed tannins and galloyl glucoses at high pH: potential impact on caterpillars. Journal of Chemical Ecology 32:2253–2267.

Barbehenn, R. V., A. Jaros, G. Lee, C. Mozola, Q. Weir, and J.-P. Salminen. 2009. Hydrolyzable tannins as "quantitative defenses": limited impact against *Lymantria dispar* caterpillars on hybrid poplar. Journal of Insect Physiology 55:297–304.

Benner, R., M. L. Fogel, E. K. Sprague, and R. E. Hodson. 1987. Depletion of ^{13}C in lignin and its implications for stable carbon isotope studies. Nature 329:708–710.

Bruno, J. F., and M. I. O'Connor. 2005. Cascading effects of predator diversity and omnivory in a marine food web. Ecology Letters 8:1048–1056.

Bryant, J. P., T. P. Clausen, P. B. Reichardt, M. C. McCarthy, and R. A. Werner. 1987. Effect of nitrogen fertilization upon the secondary chemistry and nutritional value of quaking aspen (*Populus tremuloides Michx.*) leaves for the large aspen tortrix (*Choristoneura conflictana* (Walker)). Oecologia 73:513–517.

Cardinale, B. J., D. S. Srivastava, J. Emmett Duffy, J. P. Wright, A. L. Downing, M. Sankaran, and C. Jouseau. 2006. Effects of biodiversity on the functioning of trophic groups and ecosystems. Nature 443:989–992.

Cebrian, J. 1999. Patterns in the fate of production in plant communities. American Naturalist 154:449–468.

Chen, J., R. F. Gonzalez-Laredo, and J. J. Karchesy. 2000. Minor diarylheptanoid glycosides of *Alnus rubra* bark. Phytochemistry 53:971–973.

Christensen, T. A., H. Mustaparta, and J. G. Hilderbrand. 1989. Discrimination of sex pheromone blends in the olfactory system of the moth. Chemical Senses 14:463–477.

Clark, T. 1999. Evolution and adaptive significance of larval midgut alkalinization in the insect superorder Mecopterida. Journal of Chemical Ecology 25:1945–1960.

Coley, P. D. 1980. Effects of leaf age and plant life history patterns on herbivory. Nature 284:2.

Coley, P. D., J. P. Bryant, and F. S. Chapin III. 1985. Resource availability and plant antiherbivore defense. Science 230:895–899.

Crutsinger, G. M., M. D. Collins, J. A. Fordyce, Z. Gompert, C. C. Nice, and N. J. Sanders. 2006. Plant genotypic diversity predicts community structure and governs an ecosystem process. Science 313:966–968.

Farrand, L., J. Y. Kim, S. Byun, A. Im-aram, J. Lee, J. Y. Suh, K. W. Lee, H. J. Lee, and B. K. Tsang. 2014. The diarylheptanoid hirsutenone sensitizes chemoresistant ovarian cancer cells to cisplatin via modulation of apoptosis-inducing factor and X-linked inhibitor of apoptosis. Journal of Biological Chemistry 289:1723–1731.

González-Hernández, M. P., E. E. Starkey, and J. Karchesy. 2000. Seasonal variation in concentrations of fiber, crude protein, and phenolic compounds in leaves of red alder (*Alnus rubra*): nutritional implications for cervids. Journal of Chemical Ecology 26:293–301.

González-Laredo, R. F., R. F. Helm, J. Chen, and J. J. Karchesy. 1998. Two acylated diarylheptanoid glycosides from red alder bark. Journal of Natural Products 61:1292–1294.

Hunter, M. D., and J. N. McNeil. 1997. Host-plant quality influences diapause and voltinism in a polyphagous insect herbivore. Ecology 78:977–986.

Ives, A. R., and S. R. Carpenter. 2007. Stability and diversity of ecosystems. Science 317:58–62.

Jackrel, S. L., and J. T. Wootton. 2014. Local adaptation of stream communities to intraspecific variation in a terrestrial ecosystem subsidy. Ecology 95:37–43.

Jackrel, S. L., and J. T. Wootton. 2015. Cascading effects of induced terrestrial plant defences on aquatic and terrestrial ecosystem function. Proceedings of the Royal Society of London B: Biological Sciences 282:20142522.

Karonen, M., J. Parker, A. Agrawal, and J.-P. Salminen. 2010. First evidence of hexameric and heptameric ellagitannins in plants detected by liquid chromatography/electrospray ionisation mass spectrometry. Rapid Communications in Mass Spectrometry 24:3151–3156.

Kind, T., and O. Fiehn. 2007. Seven Golden Rules for heuristic filtering of molecular formulas obtained by accurate mass spectrometry. BMC Bioinformatics 8:105.

Kinney, K. K., R. L. Lindroth, S. M. Jung, and E. V. Nordheim. 1997. Effectts of CO_2 and NO_3—availability on deciduous trees: phytochemistry and insect performance. Ecology 78:215–230.

Knight, T. M., M. W. McCoy, J. M. Chase, K. A. McCoy, and R. D. Holt. 2005. Trophic cascades across ecosystems. Nature 437:880–883.

Lankau, R. A. 2007. Specialist and generalist herbivores exert opposing selection on a chemical defense. New Phytologist 175:176–184.

Mason, C., K. Rubert-Nason, R. Lindroth, and K. Raffa. 2015. Aspen defense chemicals influence midgut bacterial community composition of gypsy moth. Journal of Chemical Ecology 41:75–84.

Mattson, W. J. 1980. Herbivory in relation to plant nitrogen content. Annual Review of Ecology and Systematics 11:119–161.

McCutcheon, A. R., S. M. Ellis, R. E. W. Hancock, and G. H. N. Towers. 1994. Antifungal screening of medicinal plants of British Columbian native peoples. Journal of Ethnopharmacology 44:157–169.

Moilanen, J., and J.-P. Salminen. 2008. Ecologically neglected tannins and their biologically relevant activity: chemical structures of plant ellagitannins reveal their in vitro oxidative activity at high pH. Chemoecology 18:73–83.

Moilanen, J., J. Sinkkonen, and J.-P. Salminen. 2013. Characterization of bioactive plant ellagitannins by chromatographic, spectroscopic and mass spectrometric methods. Chemoecology 23:165–179.

Muilenburg, V. L., P. L. Phelan, P. Bonello, and D. A. Herms. 2011. Inter- and intra-specific variation in stem phloem phenolics of paper birch (*Betula papyrifera*) and European white birch (*Betula pendula*). Journal of Chemical Ecology 37:1193–1202.

Nakagawa, S., and H. Schielzeth. 2013. A general and simple method for obtaining R^2 from generalized linear mixed-effects models. Methods in Ecology and Evolution 4:133–142.

Nakano, S., and M. Murakami. 2001. Reciprocal subsidies: dynamic interdependence between terrestrial and aquatic food webs. Proceedings of the National Academy of Sciences USA 98:166–170.

R Development Core Team. 2014. R version 3. R Project for Statistical Computing, Vienna, Austria. http://www.r-project.org

Rice, W. R., and S. D. Gaines. 1994. The ordered-heterogeneity family of tests. Biometrics 50:746–752.

Salminen, J.-P., and M. Karonen. 2011. Chemical ecology of tannins and other phenolics: we need a change in approach. Functional Ecology 25:325–338.

Sati, S. C., N. Sati, and O. P. Sati. 2011. Bioactive constituents and medicinal importance of genus *Alnus*. Pharmacognosy Reviews 5:174–183.

Schimel, J., R. Cates, and R. Ruess. 1998. The role of balsam poplar secondary chemicals in controlling soil nutrient dynamics through succession in the Alaskan taiga. Biogeochemistry 42:221–234.

Schweitzer, J. A., J. K. Bailey, B. J. Rehill, G. D. Martinsen, S. C. Hart, R. L. Lindroth, P. Keim, and T. G. Whitham. 2004. Genetically based trait in a dominant tree affects ecosystem processes. Ecology Letters 7:127–134.

Schweitzer, J., et al. 2008. From genes to ecosystems: the genetic basis of condensed tannins and their role in nutrient regulation in a populus model system. Ecosystems 11:1005–1020.

Stevens, M., A. Gusse, and R. Lindroth. 2014. Root chemistry in *Populus tremuloides*: effects of soil nutrients, defoliation, and genotype. Journal of Chemical Ecology 40:31–38.

Stout, R., W. Taft, and R. Merrit. 1985. Patterns of macroinvertebrate colonization on fresh and senescent alder leaves in two Michigan streams. Freshwater Biology 15:7.

Sunnerheim, K., and K. Bratt. 2004. Identification of centrolobol as the platyphylloside metabolite responsible for the observed effect on in vitro digestibility of hay. Journal of Agricultural and Food Chemistry 52:5869–5872.

Teece, M. A., and M. L. Fogel. 2007. Stable carbon isotope biogeochemistry of monosaccharides in aquatic organisms and terrestrial plants. Organic Geochemistry 38:458–473.

Thompson, J. N. 2005. The geographic mosaic of coevolution. University of Chicago Press, Chicago, Illinois, USA.

Vannote, R. L., G. W. Minshall, K. W. Cummins, J. R. Sedell, and C. E. Cushing. 1980. The river continuum concept. Canadian Journal of Fisheries and Aquatic Sciences 37:8.

Violle, C., B. J. Enquist, B. J. McGill, L. Jiang, C. H. Albert, C. Hulshof, V. Jung, and J. Messier. 2012. The return of the variance: intraspecific variability in community ecology. Trends in Ecology & Evolution 27:244–252.

Whitham, T. G., et al. 2006. A framework for community and ecosystem genetics: from genes to ecosystems. Nature Reviews Genetics 7:24.

Wright, M. S., and A. P. Covich. 2005. Relative importance of bacteria and fungi in a tropical headwater stream: leaf decomposition and invertebrate feeding preference. Microbial Ecology 49:536–546.

Supporting Information

Additional supporting information may be found in the online version of this article at http://onlinelibrary.wiley.com/doi/10.1890/15-1763.1/suppinfo

Appendix S1: Summary of chemical characterizations and structure drawings for thirty-five secondary metabolites.

Figure S1. Structures of ellagitannins with five side chains, R1 - R5, including a hydrogen atom (H), galloyl group (G) or hexahydroxydiphenoyl (HHDP) attached to the core glucose molecule. Side chain assignments are the most probable, but not definitive, positions.

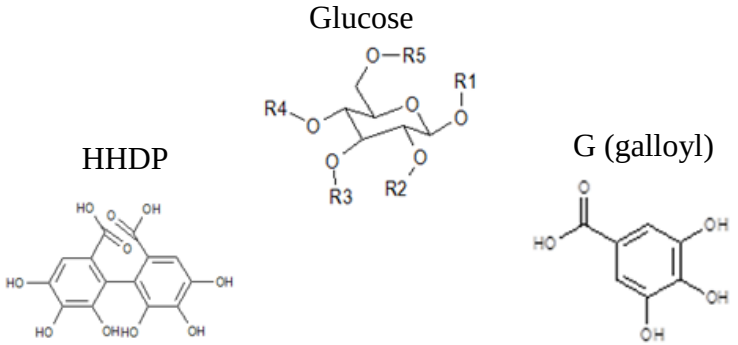

Peak	Compound	R1	R2	R3	R4	R5	Notes
3	HHDP-glucose	H	HHDP		H	H	
4	HHDP-glucose	H	H	H	HHDP		
5	galloyl-glucose						Multiple possible locations of galloyl
6	di-HHDP-glucose	H	HHDP		HHDP		Consistent with Pedunculagin β hydroxy
7	di-HHDP-glucose	H	HHDP		HHDP		Consistent with Pedunculagin α hydroxy
8	HHDP-galloyl-glucose	G	HHDP		H	H	Consistent with Isostrictinin
9	di-galloyl-HHDP-glucose	H	G	G	HHDP		Consistent with Tellimagrandin I β hydroxy
10	HHDP-galloyl-glucose	G	H	H	HHDP		Consistent with Strictinin
12	di-galloyl-HHDP-glucose	H	G	G	HHDP		Consistent with Tellimagrandin I α hydroxy
15	di-HHDP-galloyl-glucose	G	HHDP		HHDP		Consistent with Casuarictin
16	di-HHDP-galloyl-glucose	G	HHDP		HHDP		
18	tri-O-galloyl-HHDP-glucose	G	HHDP		G	G	Possibly β galloyl
22	tri-O-galloyl-HHDP-glucose	G	G	G	HHDP		Possibly α galloyl

Figure S2. Structures of diarylheptanoids with three side chains, R1-R3, including a hydrogen atom (H), hydroxyl group (OH) or other side chains attached to the core molecule.

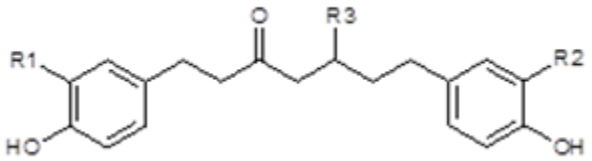

Peak	Compound	R1	R2	R3
23	Hirstunanonol-glycoside	OH	OH	O-β-D-glucopyranoside
24	Oregonin	OH	OH	O-β-D-xyloside
24a	Related to Alnuside B	H	OH	O-β-D-glucoside
26	Alnuside A	H	OH	O-β-D-xyloside
27	Alnuside B	OH	H	O-β-D-xyloside
30	Methylhirsutanonol	OH	OH	O-CH3
31	Platyphylanonol-xyloside	H	H	O-β-D-xyloside
32	Hirsutanone	OH	OH	H
34	Related to Alnuside C	OH	OH	O-2-butenoyl-β-D-glucopyranoside
35	Alnuside C	OH	OH	O-2-butenoyl-β-D-xylopyranoside

Table S1. Compound characterizations (including tentative identifications where possible), retention time, exact mass, diagnostic ions, metabolomics confidence score, references, and mean fraction (± 1 SD) base peak chromatogram ion counts per milligram of red alder leaves of thirty-five secondary metabolites found in a population of forty trees in NW Washington.

Peak	RT (secs)	TIC % Area	M-H (%)	Exact Mass	Diff (ppm)	Diagnostic ions/TIC% first	second	third	fourth	Refs	Annotation Level[6]	Chemical ID, formula (MH-) and (oxidation activity abs/s/mM)
1	115	1.7 ± 1.2				122.92/100	206.88/50				4	
2	140	5.7 ± 2.6				191.05/100	267.15/20	405.09			4	
3	200	2.0 ± 1.5	481.0612 (25)	481.0624	-1.18	300.9976/100				1,2	3	HHDP-Glucose, $C_{20}H_{17}O_{14}$ (3)
4	270	1.2 ± 0.80	481.0632 (25)	481.0624	+0.82	300.9998/100				1,2	3	HHDP-Glucose, $C_{20}H_{17}O_{14}$ (3)
5	510	0.28 ± 0.21	331.0636 (100)	331.0612	-3.47	169.0119/60				1,2	3	galloyl glucose, $C_{13}H_{15}O_{10}$ (0)
6	1100	7.4 ± 3.3	783.0726 (80)	783.0668	+3.95	300.99/100	481.0658	301.0015	169.0147	1,2	3	di-HHDP-glucose, (Pedunculagin β), $C_{34}H_{23}O_{22}$ (5)
7	1190	9.8 ± 2.5	783.0699 (80)	783.0668	+1.25	300.99/100	481.0632	301	169.0147	1,2	3	di-HHDP-glucose (Pedunculagin α), $C_{34}H_{23}O_{22}$ (5)
8	1250	3.1 ± 0.61	633.0739 (25)	633.0733	+0.56	300.9908/100	275.01/20			1,2	3	HHDP-galloyl-glucose (Isostrictinin), $C_{27}H_{21}O_{18}$ (4.9)
9	1295	5.0 ± 0.73	785.0797 (80)	785.0843	-4.60	300.99/100	275.0213/25	829.07/10		1,2	3	di-galloyl-HHDP-glucose(Tellimagrandin Iβ),$C_{34}H_{25}O_{22}$ (3.3)
10	1370	4.8 ± 1.4	633.0726 (25)	633.0733	-0.74	300.9908/100	275.01/20			1,2	3	HHDP-galloyl-glucose (Strictinin), $C_{27}H_{21}O_{18}$ (3)
11	1401	1.4 ± 0.51	965.0825 (4)			124.0154/100	183.029/15	300.9998/13	783.0692		4	too small, but major galloyl in +
12	1427	3.7 ± 1.2	785.0882 (86)	785.0855	+3.90	300.9978/100	483.0692/2	481.0516/0.3	169.01285/12	1,2	3	di-galloyl-HHDP-glucose(Tellimagrandin Iα),$C_{34}H_{25}O_{22}$ (3.3)
13	1445	1.5 ± 0.31	965.0748 (2)			300.99/100	169.0136/35	483.0728/27	635.0744/3		4	
14	1467	2.0 ± 2.2				191.0529/100	375.0607/14	633.0561/1	729.1375/1		4	derivative of chlorogenic acid
15	1491	4.9 ± 0.94	935.0857 (57)	935.0737	-1.8	300.99/100	785.0676/2	633.0622/14	169.01/3	1,2	3	di-HHDP-galloyl-glucose β (Casuarictin), $C_{41}H_{27}O_{26}$ (4.1)
16	1525	1.7 ± 0.43	935.0789 (21)	935.0737	0.7	300.99/100	785.0723/2	633.0656/10	169.0128/4	1,2	3	di-HHDP-galloyl-glucose α, $C_{41}H_{27}O_{26}$ (4.1)
17	1550	1.3 ± 0.24				300.99/100	169.013/55	635.0781/8	465.0605/12		4	
18	1570	3.1 ± 1.3	937.0929 (39)	937.0952	-2.35	300.99/100	767.0562/2	465.0658/9	169.0141/20	1,2	3	tri-O-galloyl-HHDP-glucose (β?), $C_{41}H_{29}O_{26}$ (2)
19	1610	3.0 ± 1.0	1025.07 (2)			300.99/100	191/15	169/6			4	derivative of chlorogenic acid
20	1675	1.3 ± 0.52				300.99/100					4	
21	1705	1.7 ± 0.28	997.08 (4)			300.99/100	617.06/4	757.077/8	169.01/10		4	
22	1740	1.7 ± 0.64	937.0961 (17)	937.0952	+0.85	300.99/100	785.0707/2	465.0562/3	169.0152/12	1,2	3	tri-O-galloyl-HHDP-glucose (α?), $C_{41}H_{29}O_{26}$ (2)
23	1780	1.1 ± 0.89	507.1871 (17)	507.1872	-0.09	205.0874/100	327.1249/34	121.02/90		3	2	HOG*, $C_{25}H_{31}O_{11}$
24	1840	7.8 ± 3.4	477.1751 (45)	477.1766	-1.52	205.0874/60	121.02/100	327.1249/53		3	1	Oregonin**, $C_{24}H_{29}O_{10}$
24a	1915		491.1925 (4)	491.1922	+0.23	121.0284/100	311.12/41	205.083/56	189.087/38	3,4	2	Related to Alnuside B with glucose, $C_{25}H_{30}O_{10}$
25	1960	7.6 ± 2.5	477.0666 (55)	477.0675	-0.86	301.0273/100	150.9997/24	255.0212/4	178.9932/8	5	2	Quercitin-glucuronide, $C_{21}H_{17}O_{13}$
25a	1971		463.0899 (100)	463.0882	+1.70	271.0226/89	300.024/88	301.029/51	255.0267/35	5	2	Quercitin-glucoside, $C_{21}H_{19}O_{12}$
26	2025	0.25 ± 0.29	461.1858(2)	461.1817	+4.19	311.1322	121.0308/62	205.0901/18	189.0943/6	3	2	Alnuside A, $C_{24}H_{29}O_9$
27	2060	1.3 ± 0.65	461.1837 (2)	461.1817	+1.99	311.1309	121.0303/62	205.0887/18		3	2	Alnuside B, $C_{24}H_{29}O_9$
28	2090	1.3 ± 0.65	483.012 (15)			300.99	299.9957/13				4	
29	2170	5.7 ± 2.0	447.0964 (100)	447.0933	+3.12	301.0372/61	178.9975/3	151.0024/3	283.0394/6	5	2	Quercitin-rhamnoside, $C_{21}H_{19}O_{11}$
30	2230	1.5 ± 0.98	359.1517 (1)	359.1500	+1.69	121.028/100	205.08/3	327.116/2		3	2	Methylhirsutanonol, $C_{20}H_{23}O_6$
31	2250	0.63 ± 1.1	445.1866 (1)	445.1868	-0.19	295.1349/100	189.0928/45	121.0297/10	169.0136/1	3	2	platyphylanolanol-xyloside, $C_{24}H_{30}O_8$
32	2298	1.0 ± 0.68	327.1232 (13)	327.1238	-0.60	121.031/100	205.0896/8	109.028/11		3	2	Hirsutanone, $C_{19}H_{19}O_5$
33	2310	0.26 ± 0.18	485 (0)			255.026/100	227.03/66	121.027/11	327.127/6		4	
34	2380	2.7 ± 2.0	591.2442 (4)	591.2447	-0.50	205.086/100	327.1282/44	121.02/34		4	3	novel diarylheptanoid***, $C_{30}H_{39}O_{12}$
35	2405	0.45 ± 0.62	561.2274(7)	561.2341	-1.44	205.0897/100	121/48	327.1274/32	109.029/9	4	2	Alnuside C, $C_{29}H_{37}O_{11}$

References: 1: (Moilanen et al. 2013), 2: (Gu et al. 2013), 3: (Novakavic et al. 2014), 4: (Lv and Shea 2010), 5. (Falcao et al. 2012) 6. (Sumner et al. 2007)

*HOG: 1,7-bis(3,4-dihydroxyphenyl)-5-β-D-xylopyranosyl-3-heptanone

**Oregonin: 1,7-bis(3,4-dihydroxyphenyl)-5-β-D-glycopyranosyl-3-heptanone

*** Novel diarylheptanoid: Alnuside C with glucose replacing xylose, 1,7-bis-(3,4-dihydroxy-phenyl)-5-hydroxy-3-heptanone-5-0-[2-(2-methylbutenoyl)]-β-D-glucopyranoside

References

Moilanen J, Sinkkonen J, Salminen J-P. Characterization of bioactive plant ellagitannins by chromatographic, spectroscopic and mass spectrometric methods. Chemoecology. 2013;23(3): 165-79.

Gu D, Yang Y, Bakri M, Chen Q, Xin X, Aisa HA. A LC/QTOF–MS/MS application to investigate chemical compositions in a fraction with protein tyrosine phosphatase 1B inhibitory activity from *Rosa rugosa* flowers. Phytochemical Analysis. 2013;24(6): 661-70.

Novaković M, Pešić M, Trifunović S, Vučković I, Todorović N, Podolski-Renić A, et al. Diarylheptanoids from the bark of black alder inhibit the growth of sensitive and multi-drug resistant non-small cell lung carcinoma cells. Phytochemistry. 2014;97: 46-54.

Lv H, She G. Naturally occurring diarylheptanoids. Natural Product Communications. 2010;5(10): 1687-708.

Falcão SI, Vale N, Gomes P, Domingues MRM, Freire C, Cardoso SM, et al. Phenolic profiling of Portuguese propolis by LC–MS spectrometry: Uncommon propolis rich in flavonoid glycosides. Phytochemical Analysis. 2013;24(4): 309-18.

Sumner L, Amberg A, Barrett D, Beale M, Beger R, Daykin C, et al. Proposed minimum reporting standards for chemical analysis. Metabolomics. 2007;3(3): 211-21.

Appendix S2: Leaf traits correlated with ellagitannin, diarylheptanoid and flavonoid content.

Table S1. Standardized coefficients from type III linear regression ($F_{2,37} = 13.84$, $p < 0.001$), showing the association of various leaf traits on Principal Component 1 (i.e. ellagitannin content, but see Appendix S4, Table S1). Variables excluded from the model were tree diameter, leaf thickness, %C, %P, C:N, C:P, $^{15}N/^{14}N$, and $^{13}C/^{12}C$.

Source	Estimated	t value	Pr(>|t|)
% Nitrogen	2.377	4.995	< 0.0001
Nitrogen: Phosphorus	-1.243	-2.612	0.0129

Table S2. Standardized coefficients from type III linear regression ($F_{4,35} = 10.42$, $p < 0.001$), showing leaf thickness and nutrient level is associated with Principal Component 2 (i.e. diarylheptanoid content, but see Appendix S4, Table S1). Variables excluded from the model were tree diameter, %N, %C, %P, $^{15}N/^{14}N$, and $^{13}C/^{12}C$.

Source	Estimated	t value	Pr(>|t|)
Leaf thickness	-1.167	-3.431	0.00156
Carbon: Nitrogen	4.687	3.201	0.00291
Carbon: Phosphorus	-6.983	-2.813	0.00799
Nitrogen: Phosphorus	5.741	2.537	0.0158

Table S3. Standardized coefficients from type III linear regression ($F_{3,36} = 3.46$, $p < 0.026$), showing the association of various leaf traits on Principal Component 3 (i.e. flavonoid content, but see Appendix S4, Table S1). Variables excluded from the model were tree diameter, C:N, N:P, C:P, %N, %P, and $^{13}C/^{12}C$.

Source	Estimated	t value	Pr(>|t|)
$^{15}N/^{14}N$	0.545	2.232	0.032
Leaf Thickness	-0.415	-1.709	0.096
% Carbon	-0.332	-1.372	0.18

Table S4. Standardized coefficients from best fitting stepwise linear mixed model (marginal $R^2 = 0.48$), showing ellagitannin-depleted and thin leaves are correlated with high rates of aquatic leaf decomposition in the Pysht, Little Hoko, Hoko and Sekiu Rivers. Variables excluded from the model were PC2, PC3, tree diameter, % N, % C, % P, C:N, C:P, N:P, $^{13}C/^{12}C$ and $^{15}N/^{14}N$.

Source	Estimated	t value	Pr(>|t|)
PC1 (ellagitannin content)	0.057	3.086	0.0038
Leaf thickness	-0.119	-6.543	> 0.001

Appendix S3. Illustration of experimental design for reciprocal transplant experiments

Figure S1. Five red alder trees from each of four sites, two from each river, were used to construct twenty diets. These diets were used to make diet plates containing all twenty diets. All aquatic diet plates and all riparian soil diet plates were constructed identically, but were deployed in each of the four different sites in the experimental run. Therefore, at each aquatic deployment site, there were twenty diet options made from leaves collected from twenty alder trees. For example, incubating in the water at Site 1 of the Little Hoko River were 5 diets from 5 trees growing along Site 1 of the Little Hoko, 5 diets from trees growing along Site 2 of the Little Hoko, and 10 diets from the 10 trees growing along the Pysht River. This diagram includes arrows for only one tree of five per site and for only two of the four sites, one per river, as a partial example of the complete design.

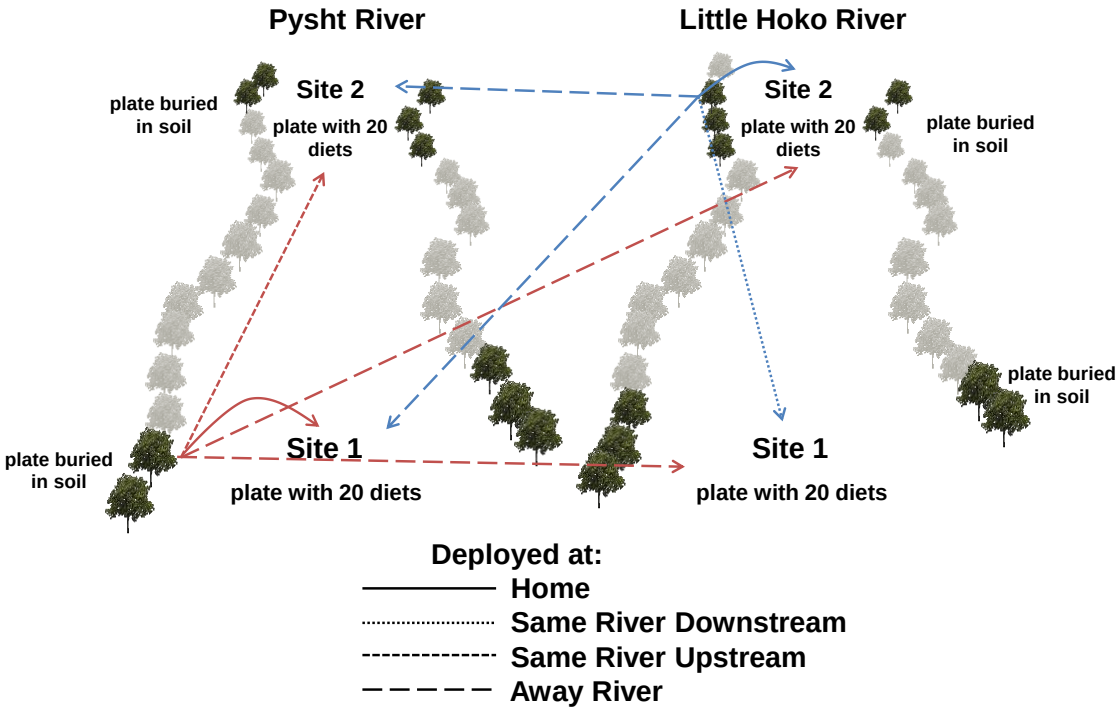

Figure S2. Twenty diets containing different red alder tree extracts deployed underwater in a 96 well plate on a stream bed.

Photo Credit: S. L. Jackrel

Figure S3. Caddisflies feeding on a diet plate deployed on a stream bed.

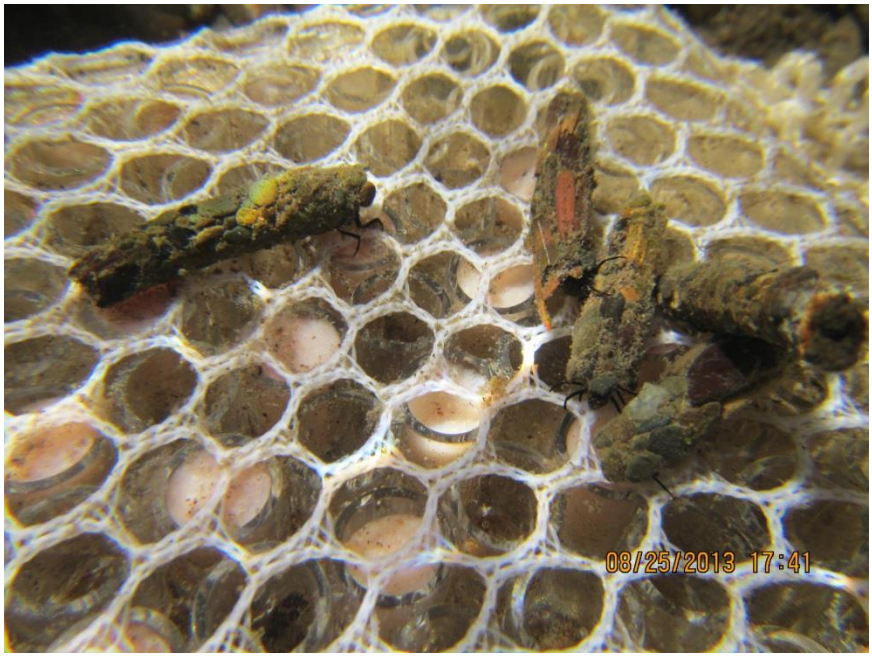

Photo Credit: S. L. Jackrel

Appendix S4: Loadings for principal component analysis

Table S1. Variation in chromatograms of secondary metabolites in leaves of a red alder population explained by differences in relative quantities of ellagitannins (PC1), relative quantities of diarylheptanoids (PC2), and relative quantities of flavonoids (PC3) using a principal component analysis. Largest PC loadings (≥ |0.20|) and listed for each component.

PC1 Cumulative % of Variance: 40.2		PC2 Cumulative % of Variance: 58.0		PC3 Cumulative % of Variance: 65.5	
HHDP-galloyl-glucose (# 10)	-0.249	HOG (#23)	0.364	quercetin-rhamnose (#29)	-0.381
# 17	-0.249	methylhirsutanonol (# 30)	0.363	# 33	-0.335
di-HHDP-galloyl-glucose α (# 16)	-0.249	hirsutanone (# 32)	0.357	HHDP-glucose (# 4)	-0.332
di-HHDP-galloyl-glucose β (# 15)	-0.248	alnuside C (glucose replaces xylose) # 34	0.345	# 1	0.332
di-galloyl-HHDP-glucose (# 9)	-0.246	alnuside C (# 35)	0.297	quercetin-glucuronide and quercetin-glucoside (# 25)	-0.315
# 13	-0.243	oregonin (# 24)	0.265	HHDP-glucose (# 3)	0.241
# 21	-0.234	platyphylanol-xylose (# 31)	0.223	# 14	-0.206
di-HHDP-glucose (# 7)	-0.228	alnuside A (# 26)	0.205		
di-galloyl-HHDP-glucose (# 12)	-0.227	# 14	0.204		
HHDP-galloyl-glucose (# 8)	-0.217				
tri-O-galloyl-HHDP-glucose (β) (# 18)	-0.209				
di-HHDP-glucose (#6)	-0.207				
# 28	-0.200				

Appendix S5: Canonical correlation coefficients and structure matrix for discriminant function analysis

Table S1. Importance of ellagitannins, diarylheptanoids and flavonoids with DF1 (shown in Fig. 4). Numbering corresponds with chromatogram peaks described in Fig 1. Bold/italics highlights four compounds that most strongly influence discriminant scores.

Chemical Compound	Standardized Canonical Coefficients	Structure Matrix
1 (unknown)	18.744	0.017
4 (HHDP-Glucose)	11.559	-0.008
5 (galloyl-glucose)	***-28.468***	0
6 (di-HHDP-glucose)	1.911	-0.011
8 (HHDP-galloyl-glucose)	-8.305	0.002
9 (di-galloyl-HHDP-glucose)	12.228	-0.009
10 (HHDP-galloyl-glucose)	***26.767***	-0.007
11 (unknown ellagitannin)	-3.514	-0.013
12 (di-galloyl-HHDP-glucose)	-12.943	-0.01
14 (unknown)	9.135	0.001
15 (di-HHDP-galloyl-glucose β)	-3.043	-0.012
16 (di-HHDP-galloyl-glucose α)	-15.62	-0.01
17 (unknown)	11.823	-0.009
18 (tri-O-galloyl-HHDP-glucose β)	19.123	-0.015
19 (unknown ellagitannin)	16.65	-0.004
20 (unknown)	-7.769	-0.004
21 (unknown)	-7.916	-0.009
22 (tri-O-galloyl-HHDP-glucose α)	***-21.657***	-0.035
23 (HOG)	***23.527***	0.012
24 (Oregonin)	14.145	0.007
26 (Alnuside A)	8.119	0.013
27 (Alnuside B)	13.512	0.01
28 (unknown)	-8.181	0
29 (Quercitin-rhamnose)	-2.437	-0.018
30 (methylhirsutanonol)	-9.896	0.018
33 (unknown diarylheptanoid)	7.007	-0.011
34 (1,7-bis-(3,4-dihydroxy-phenyl)-5-hydroxy-3-heptanone-5-0-[2-(2-methylbutenoyl)]-β-D-glucopyranoside)	-8.687	0.013

Appendix S6. Mass spectrometry data for twenty-five ellagitannins, diarylheptanoids and flavonoids.

Peak # 3:
HHDP-Glucose
m/z 481.0624, $C_{20}H_{18}O_{14}$

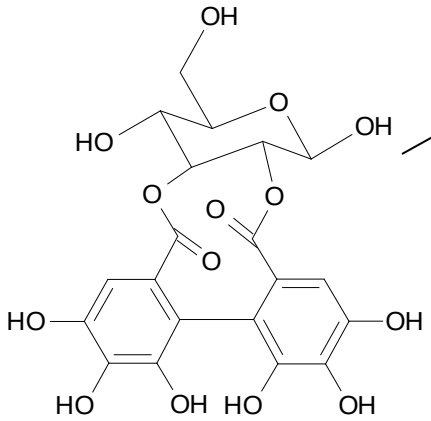

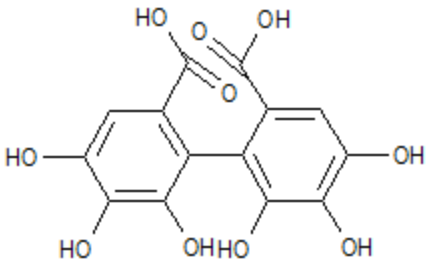

m/z 338.2298
$C_{14}H_{10}O_{10}$
(intermediate form)

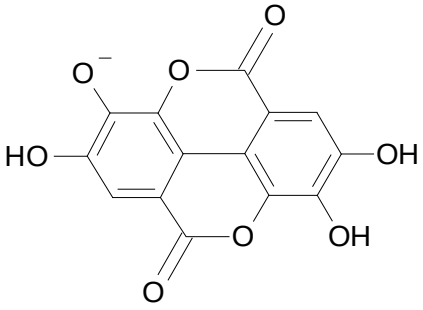

-H_2O (Gu 2013)
m/z 300.9998
$C_{14}H_5O_8$

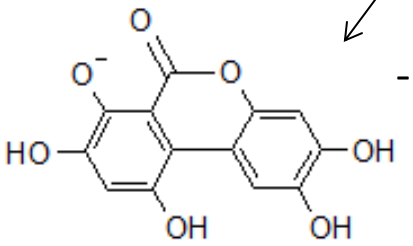

-H_2O, -CO_2 (Gu 2013)
m/z 275.0192
$C_{13}H_7O_7$

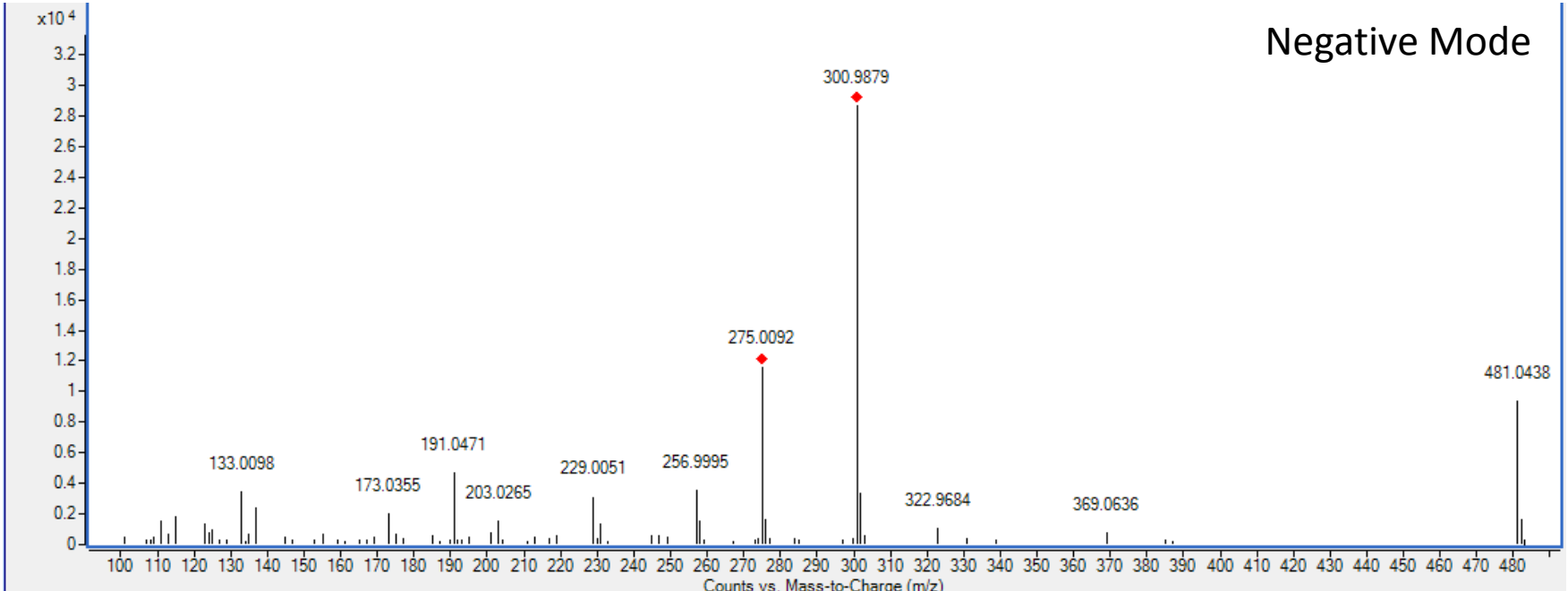

Peak # 4:
HHDP-Glucose
m/z 481.0624, $C_{20}H_{18}O_{14}$

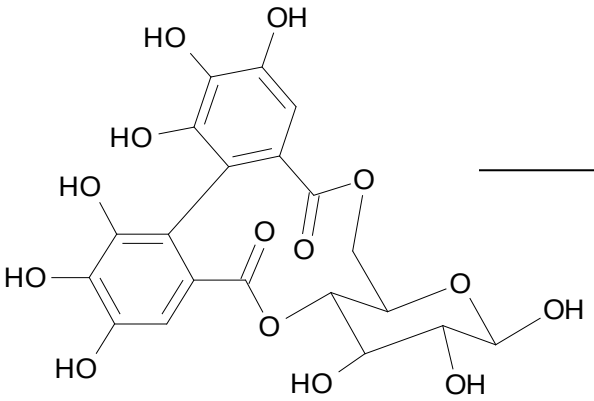

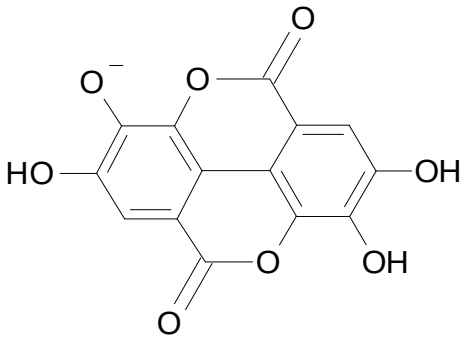

m/z 300.9998
$C_{14}H_5O_8$

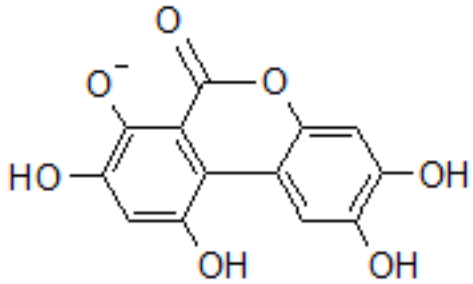

m/z 275.0192
$C_{13}H_7O_7$

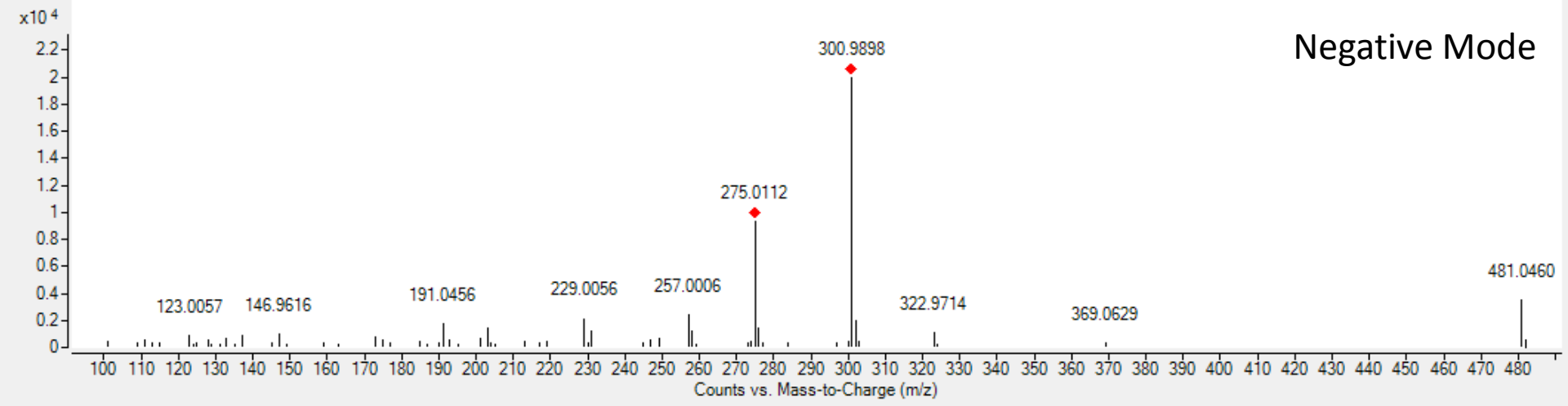

Peak # 5:

Glucose + 3G

m/z = 331.0743, $C_{13}H_{16}O_{10}$

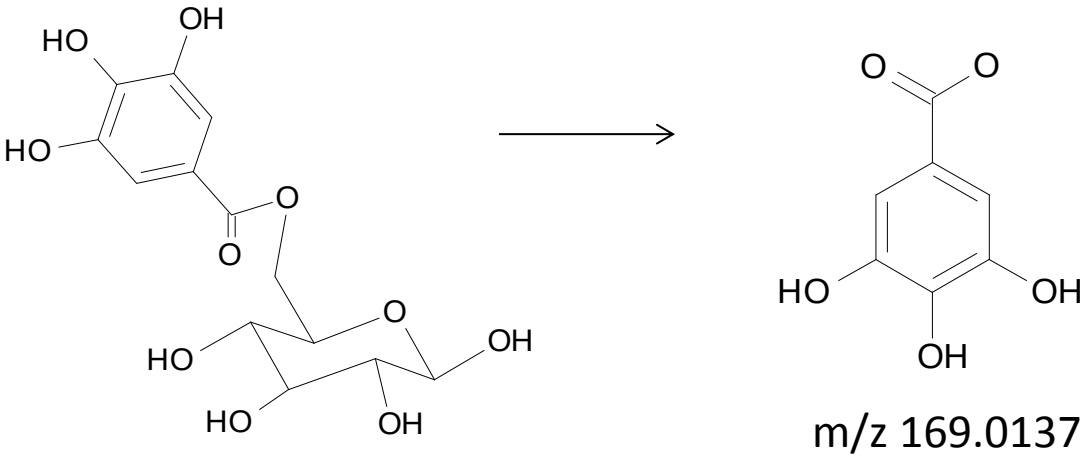

m/z 169.0137

$C_7H_5O_5$

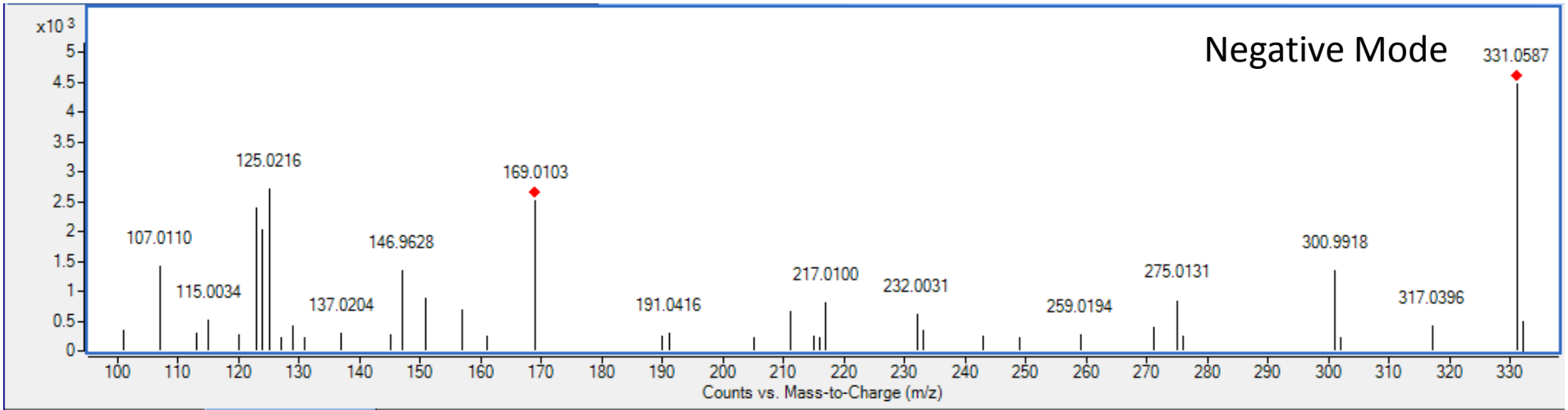

Peak # 6:

Pedunculagin β (2xHHDP + glucose)

m/z 783.0681, $C_{34}H_{23}O_{22}$

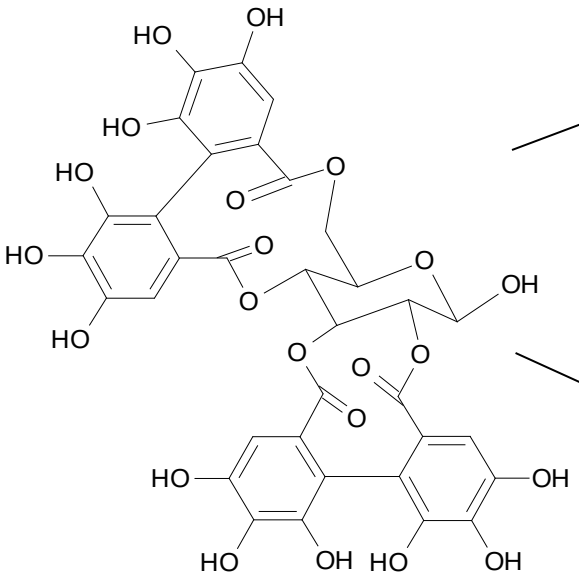

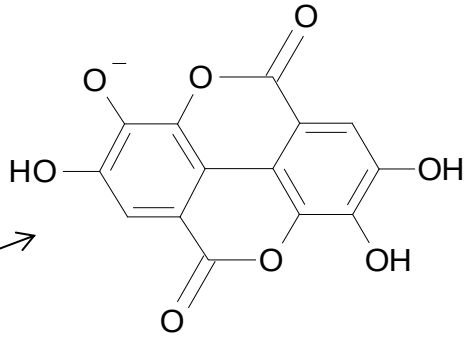

m/z 300.9998

$C_{14}H_5O_8$

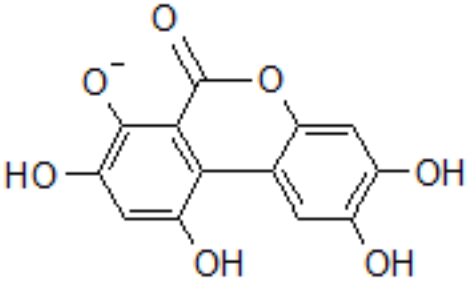

m/z 275.0192

$C_{13}H_7O_7$

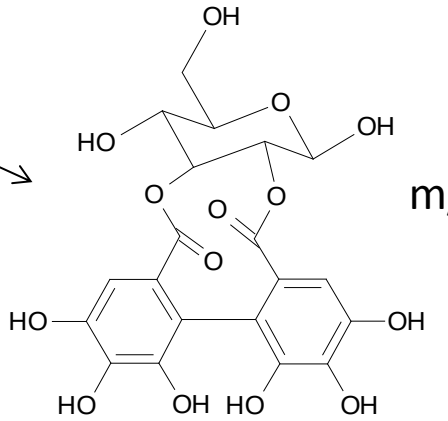

m/z 481.0624

$C_{20}H_{18}O_{14}$

Negative Mode

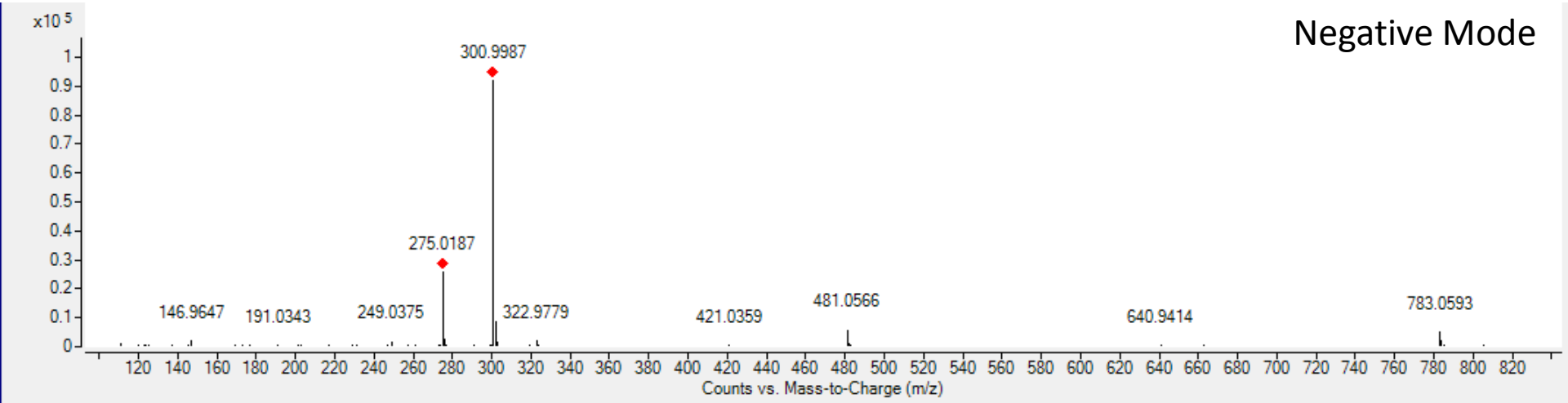

Peak # 7

Pedunculagin-α (2xHHDP + glucose)

m/z =783.0681, $C_{34}H_{23}O_{22}$

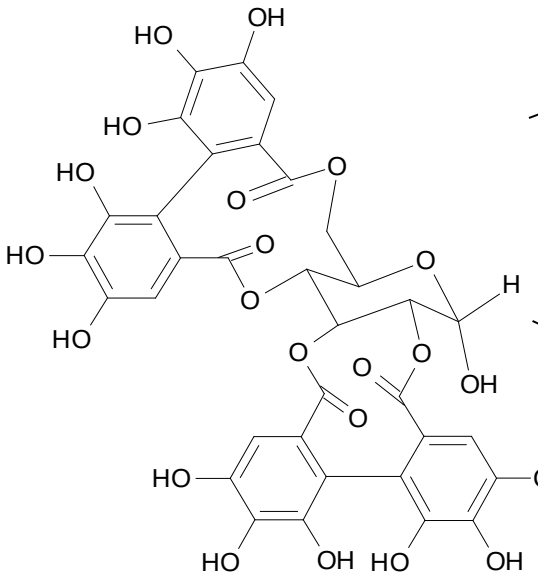

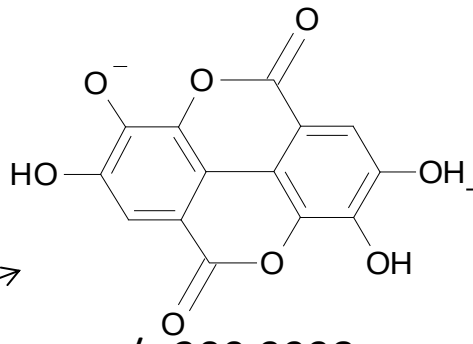

m/z 300.9998

$C_{14}H_5O_8$

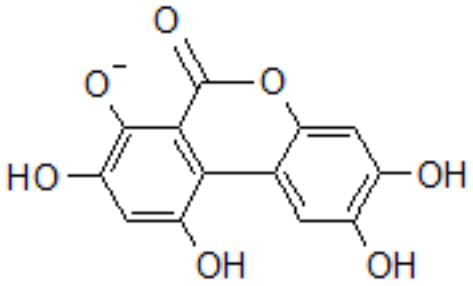

m/z 275.0192

$C_{13}H_7O_7$

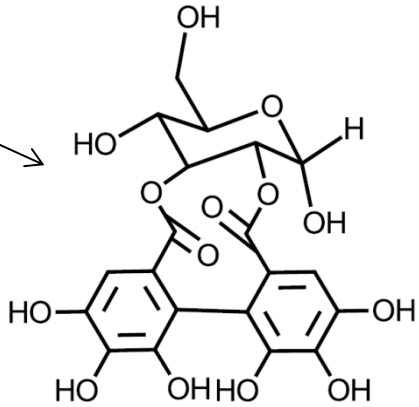

m/z 481.0624

$C_{20}H_{18}O_{14}$

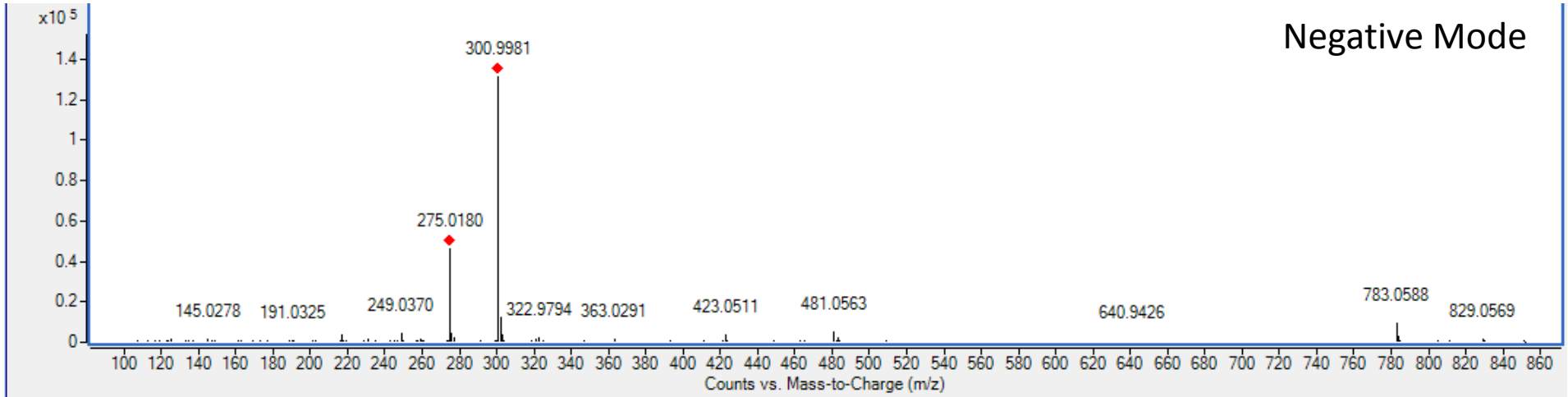

Negative Mode

Peak # 8:

Isostrictinin (1G+HHDP+glucose)

m/z 633.0733373, $C_{27}H_{22}O_{18}$

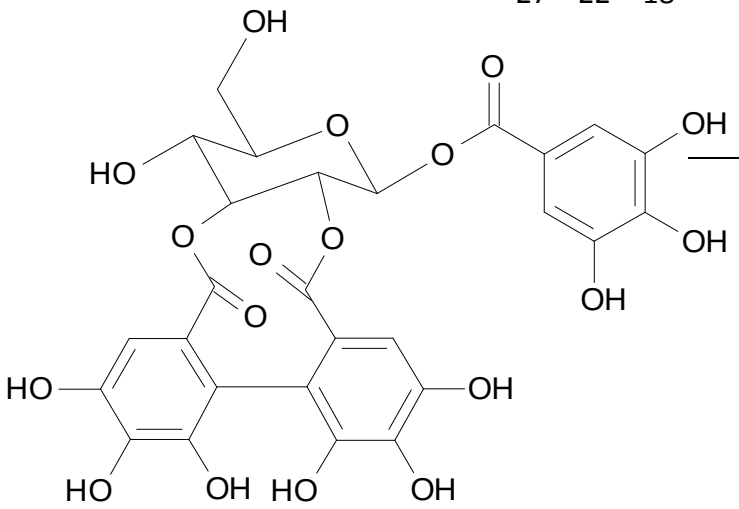

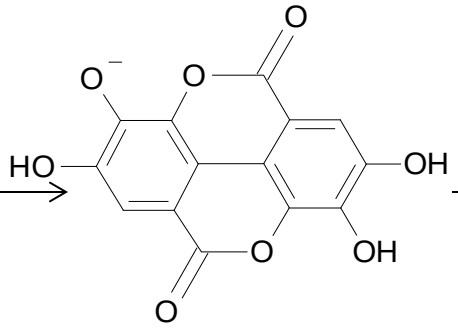

m/z 300.9998

$C_{14}H_5O_8$

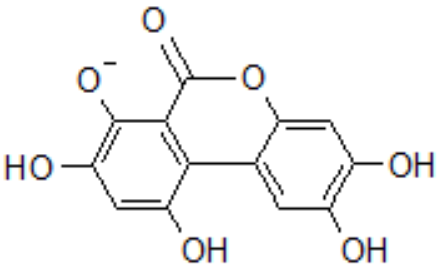

m/z 275.0192

$C_{13}H_7O_7$

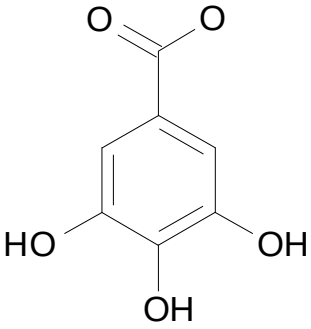

m/z 169.0137

$C_7H_5O_5$

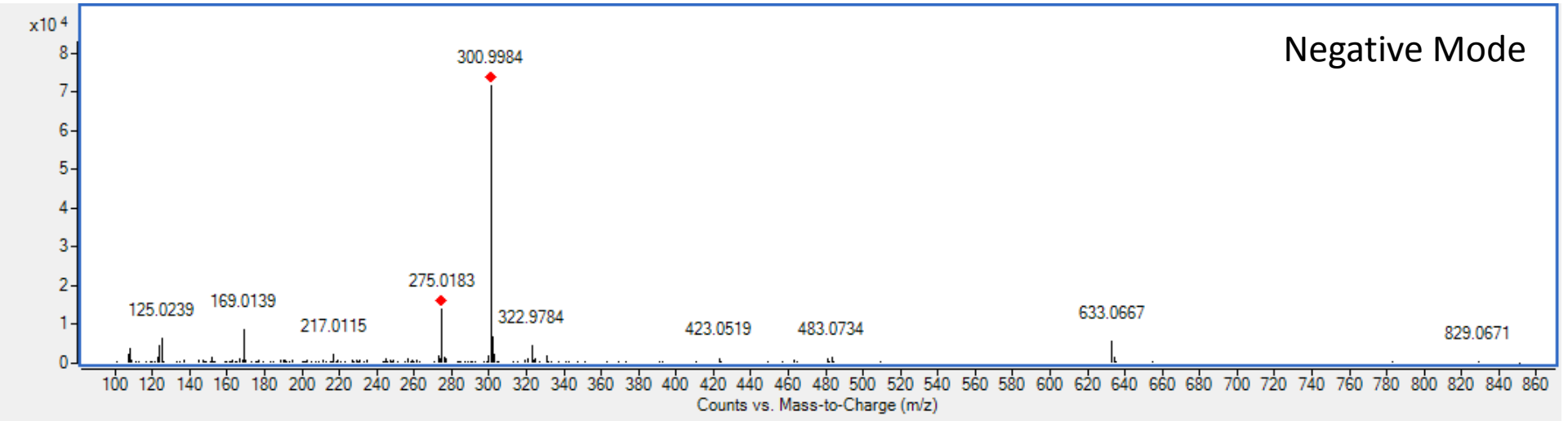

Peak # 9:

Tellimagrandin I β (HHDP+2G+glucose)

m/z 785.08429, $C_{34}H_{26}O_{22}$

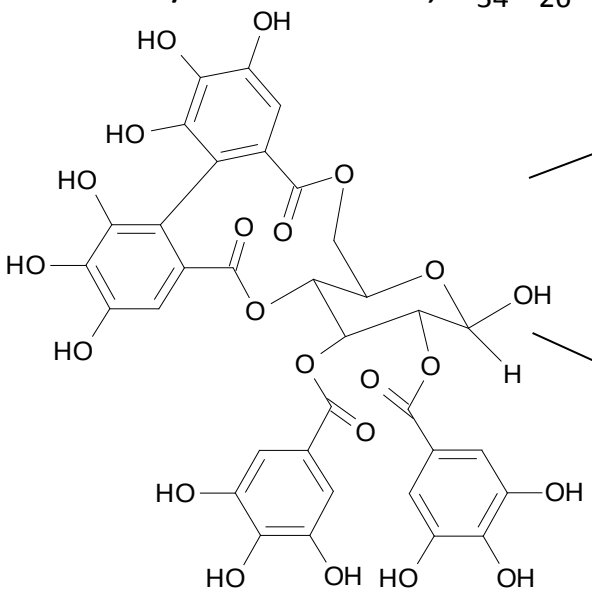

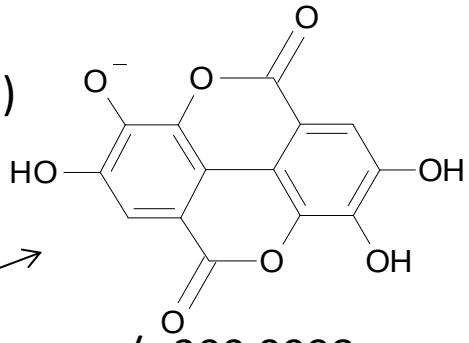

m/z 300.9998

$C_{14}H_5O_8$

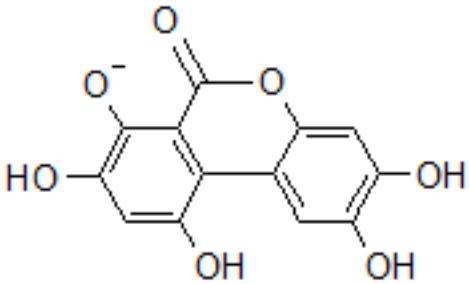

m/z 275.0192

$C_{13}H_7O_7$

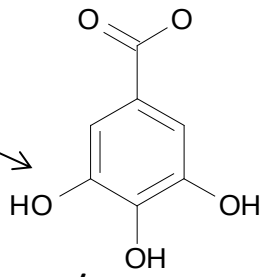

m/z 169.0137

$C_7H_5O_5$

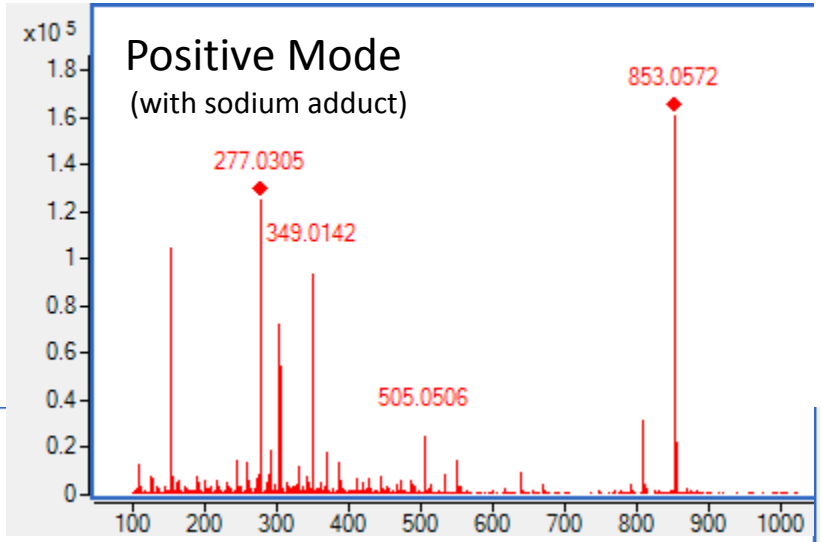

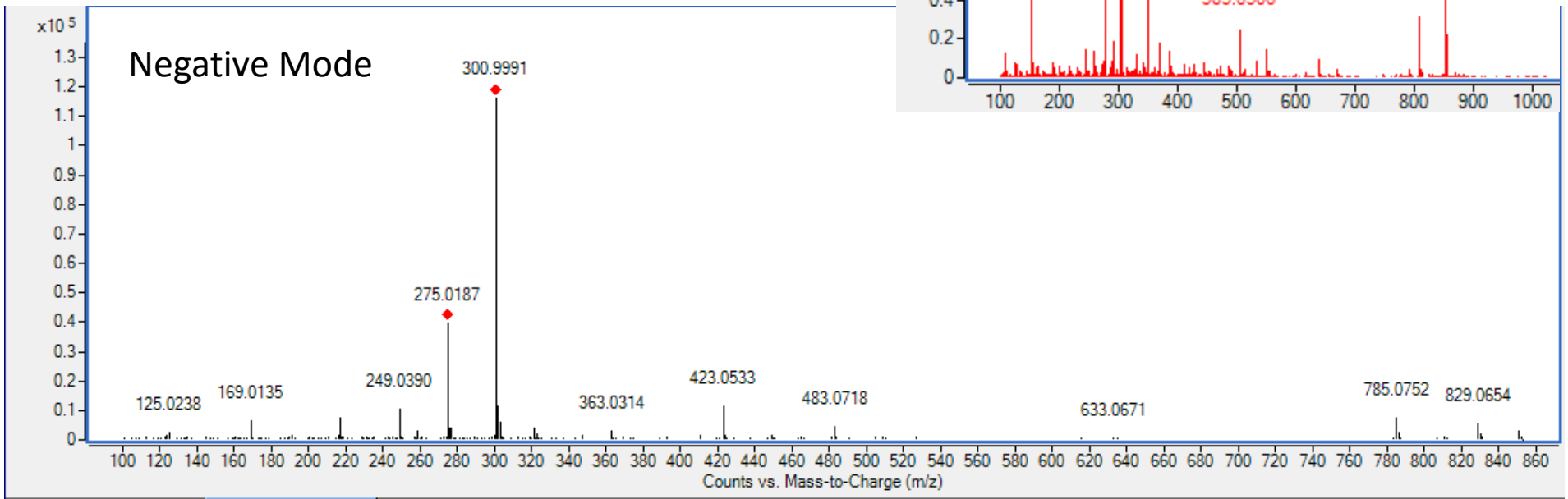

Peak # 10:
Strictinin (1G+1HHDP+glucose)
m/z 633.0733373, $C_{27}H_{22}O_{18}$

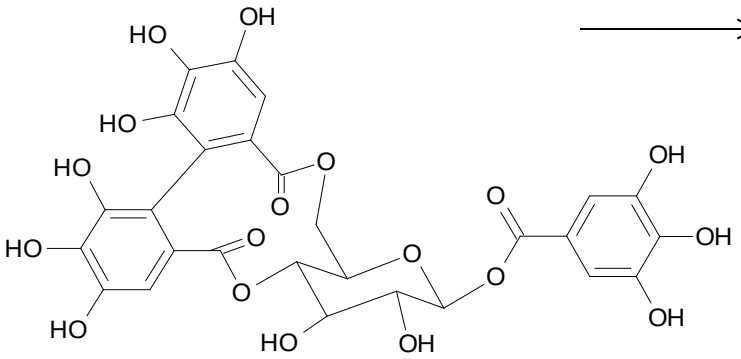

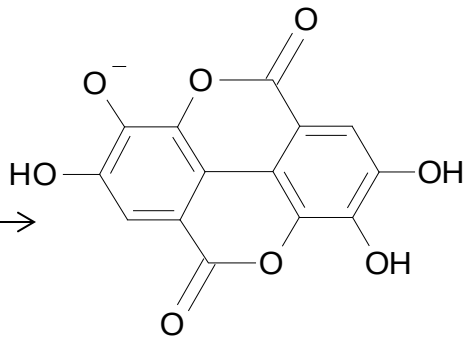

m/z 300.9998
$C_{14}H_5O_8$

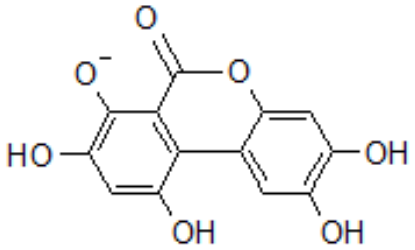

m/z 275.0192
$C_{13}H_7O_7$

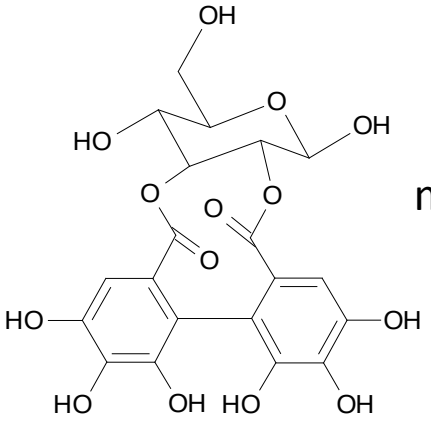

m/z 481.0624
$C_{20}H_{18}O_{14}$

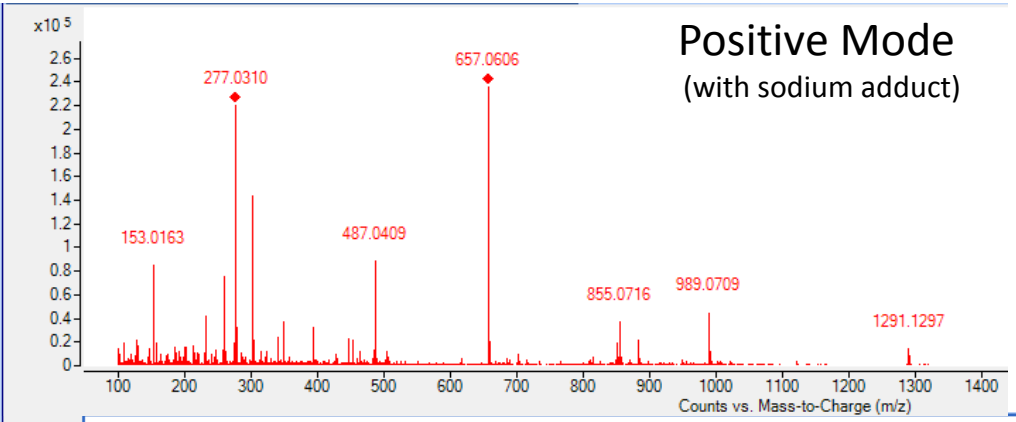

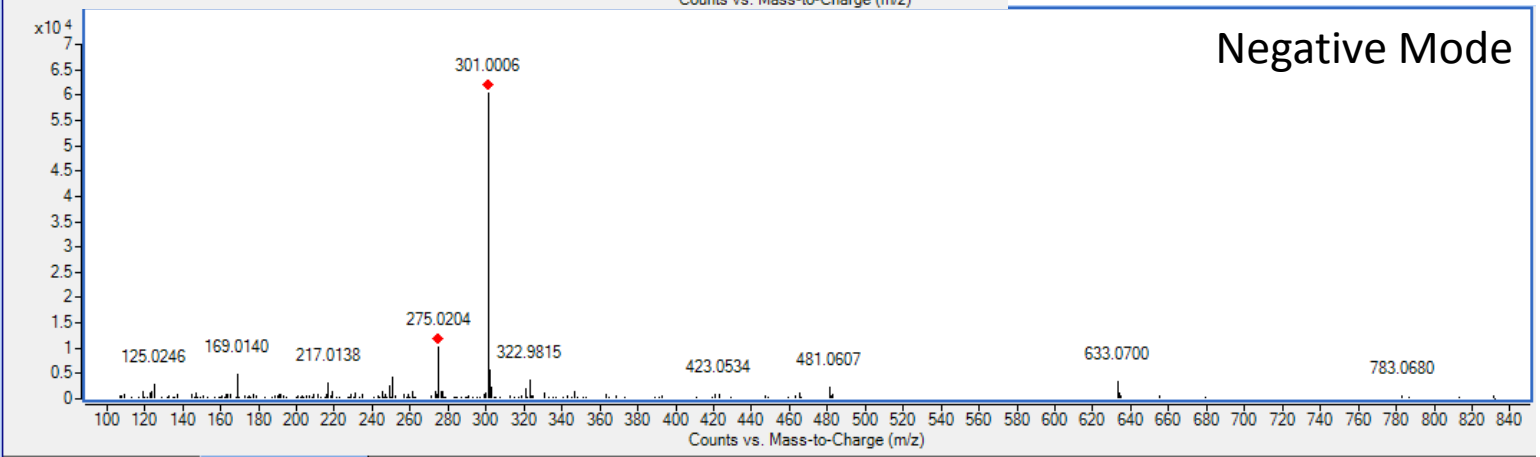

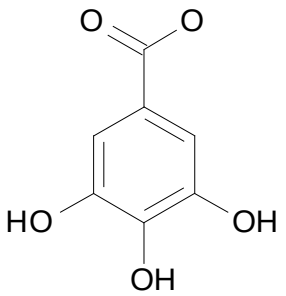

m/z 169.0137
$C_7H_5O_5$

Peak # 12:

Tellimagrandin I α (HHDP+2G+glucose)

m/z 785.08429, $C_{34}H_{26}O_{22}$

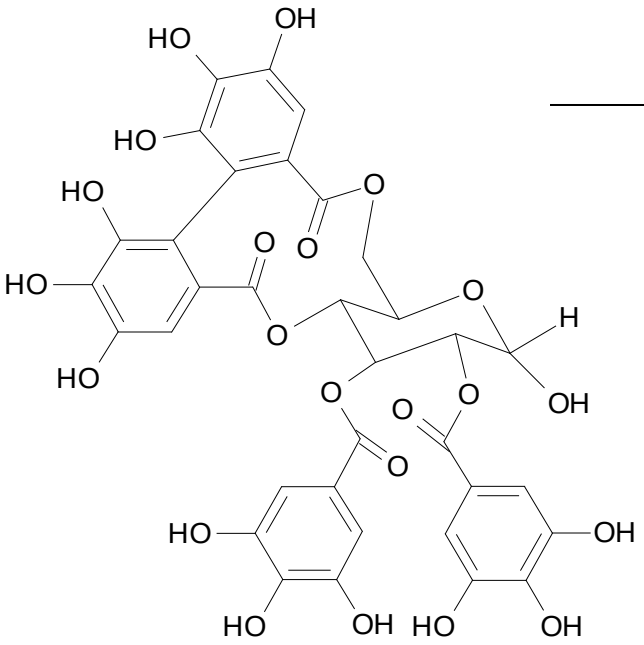

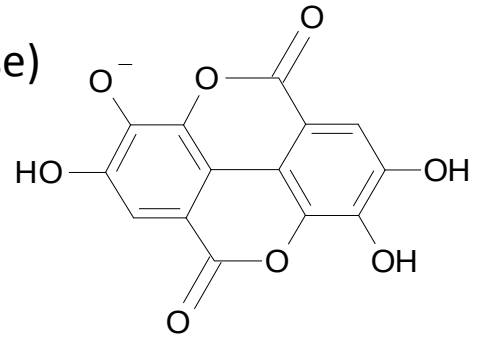

m/z 300.9998

$C_{14}H_5O_8$

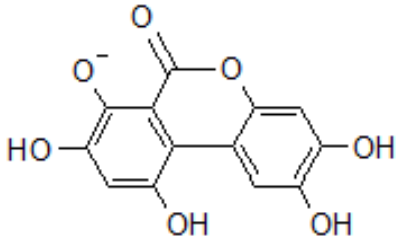

m/z 275.0192

$C_{13}H_7O_7$

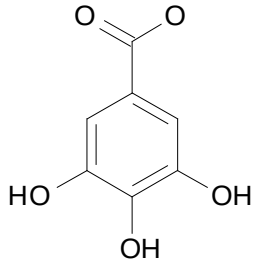

m/z 169.0137

$C_7H_5O_5$

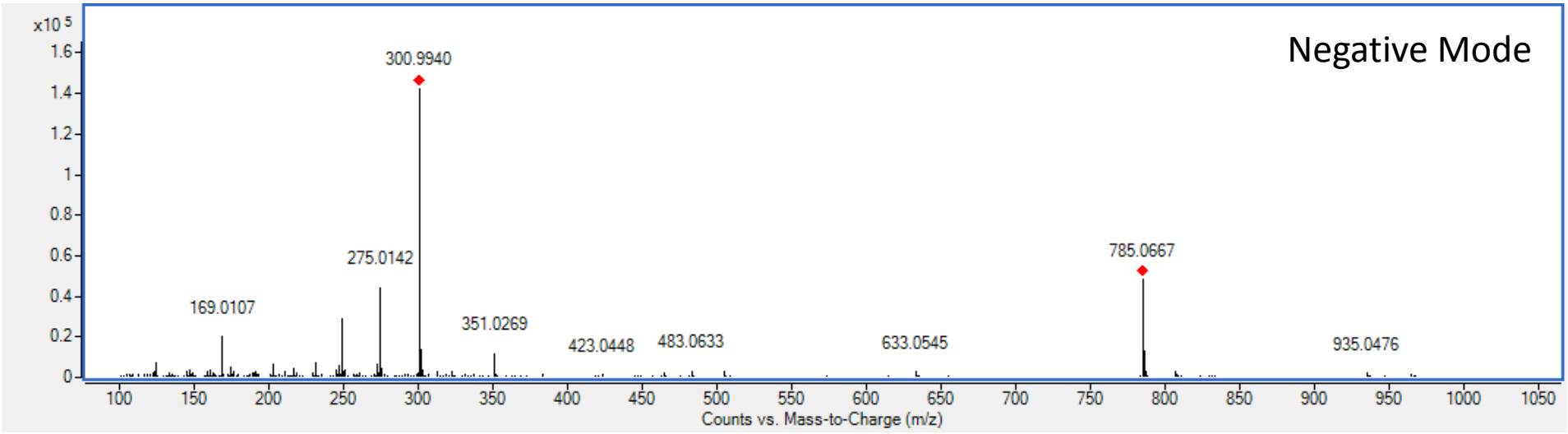

Peaks # 15 and # 16:
2xHHDP+G+ glucose
m/z 935.0737, $C_{41}H_{27}O_{26}$

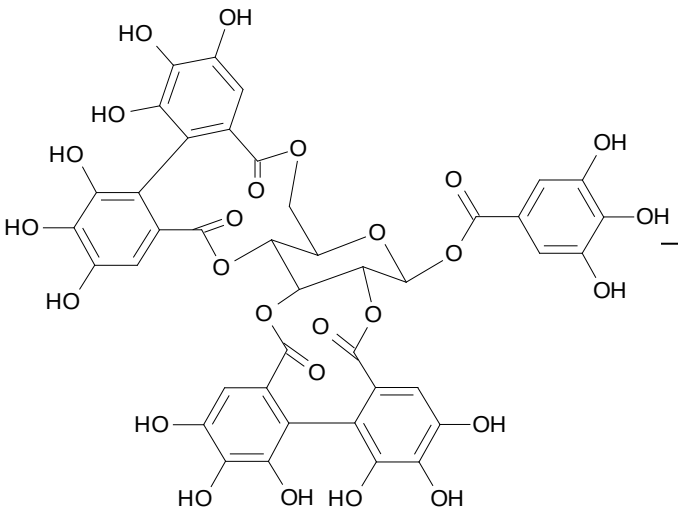

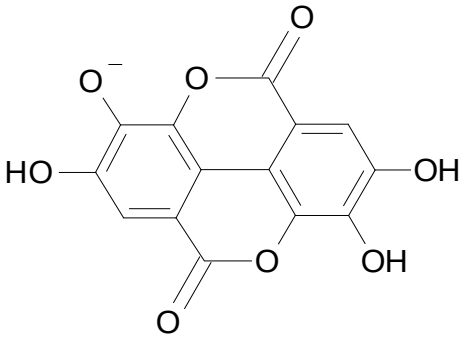

m/z 300.9998
$C_{14}H_5O_8$

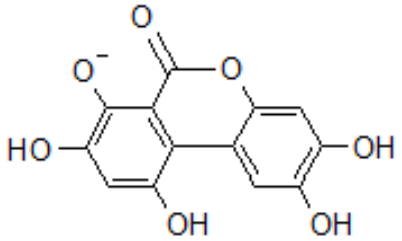

m/z 275.0192
$C_{13}H_7O_7$

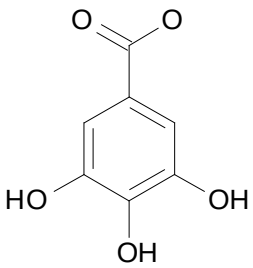

m/z 169.0137
$C_7H_5O_5$

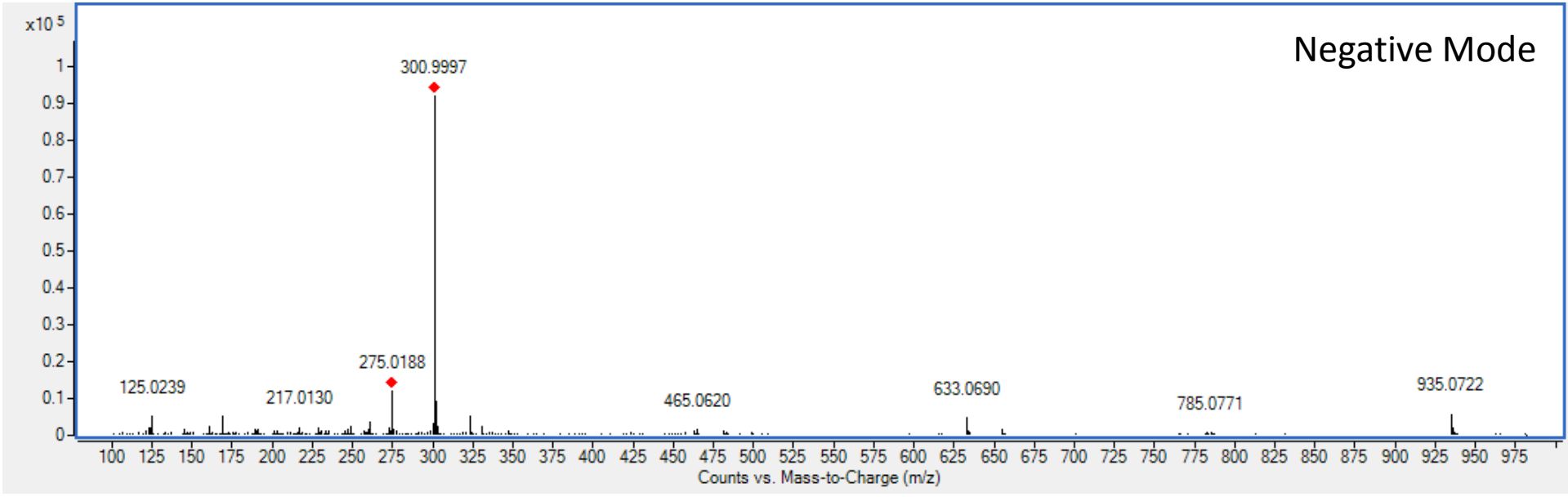

Peaks # 18 and # 22:
3G + HHDP-glucose isomers
m/z 937.0952, $C_{41}H_{29}O_{26}$

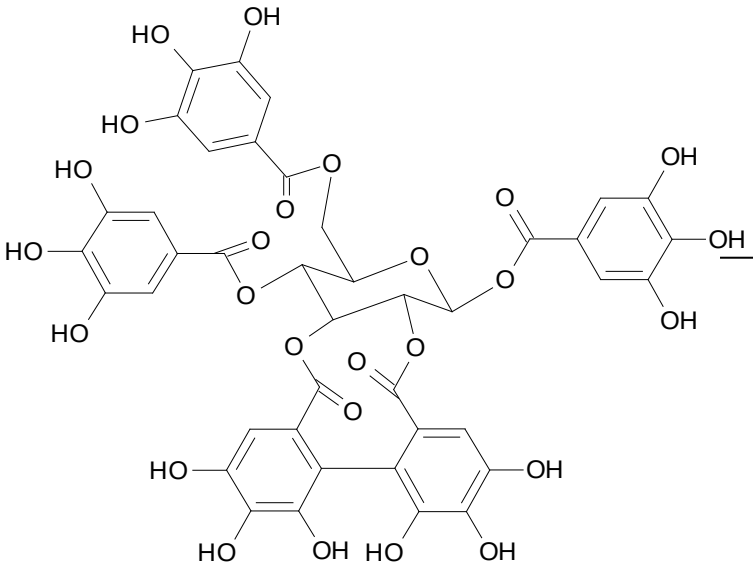

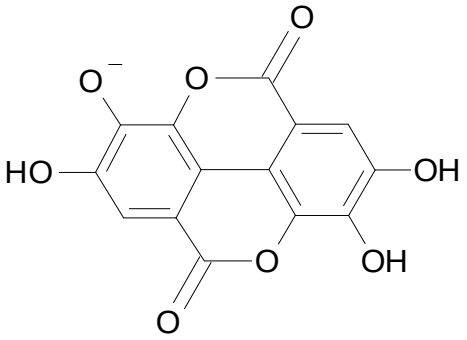

m/z 300.9998
$C_{14}H_5O_8$

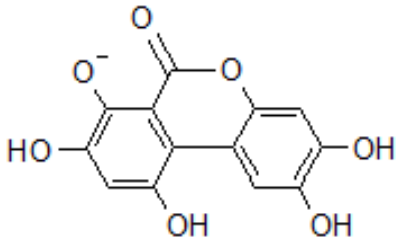

m/z 275.0192
$C_{13}H_7O_7$

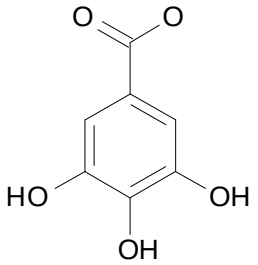

m/z 169.0137
$C_7H_5O_5$

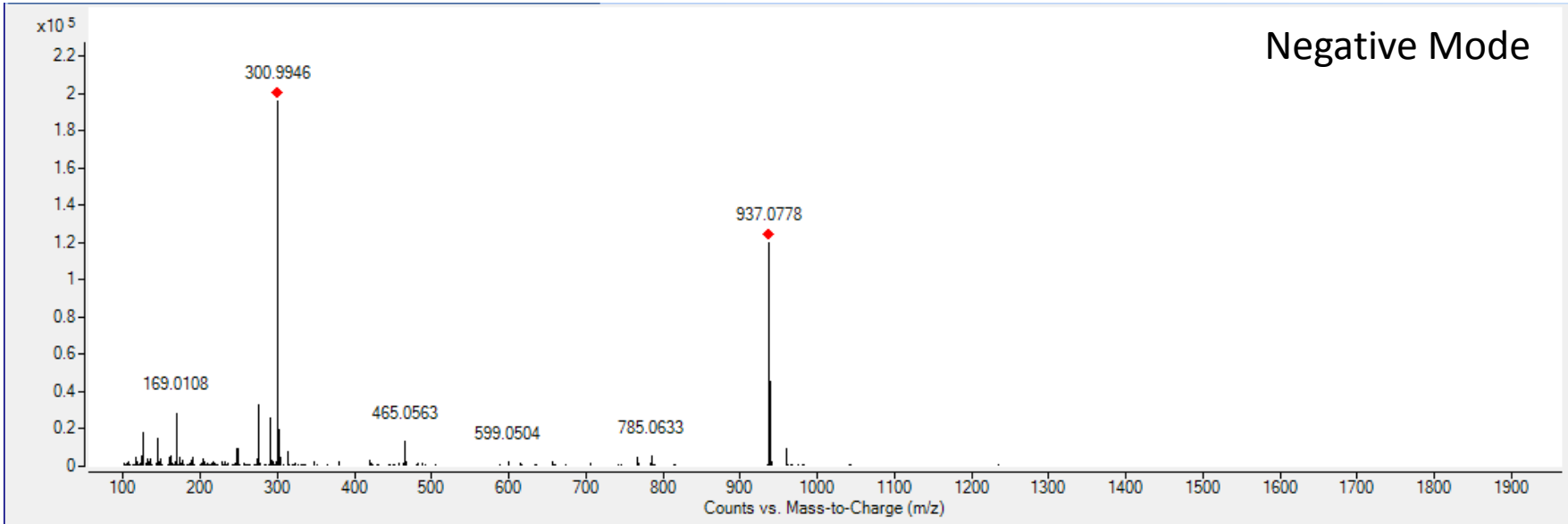

Peak # 23:

Hirsutin glucoside (HOG)

m/z 508.5272, $C_{25}H_{32}O_{11}$

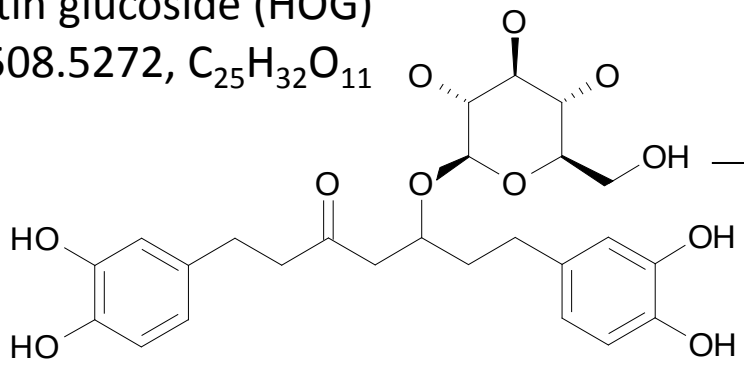

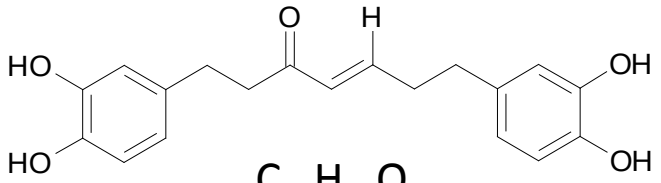

$C_{19}H_{20}O_5$

327.1311

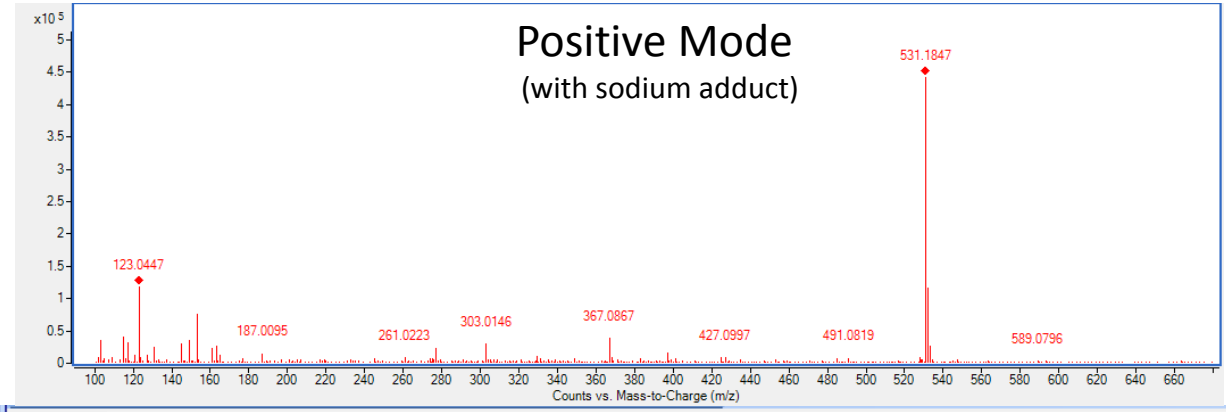

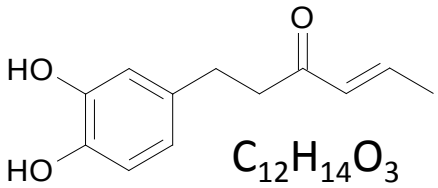

$C_{12}H_{14}O_3$

205.0943

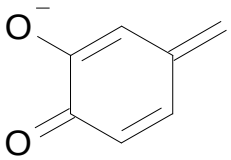

$C_7H_5O_2$

121.0290

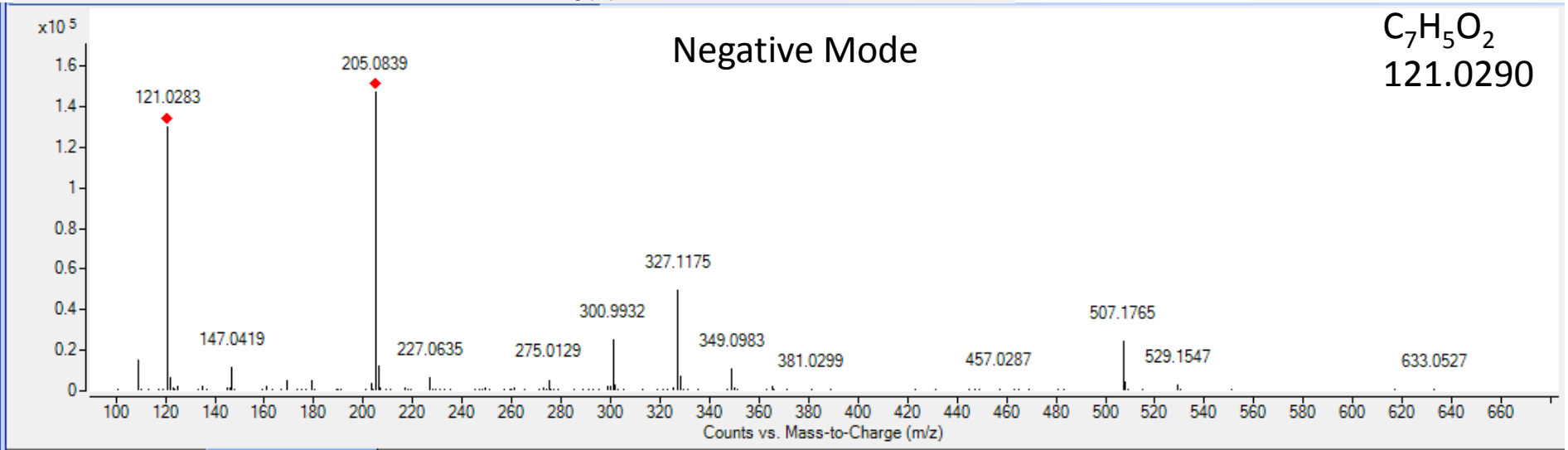

Peak # 24:

Oregonin xyloside

m/z 478.5007, $C_{24}H_{30}O_{10}$

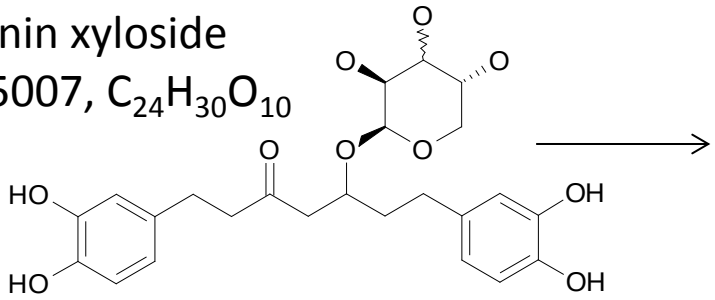

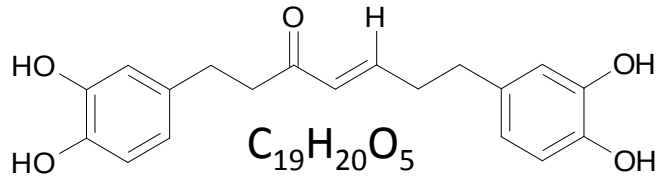

$C_{19}H_{20}O_5$

327.1311

Positive Mode

(with sodium adduct)

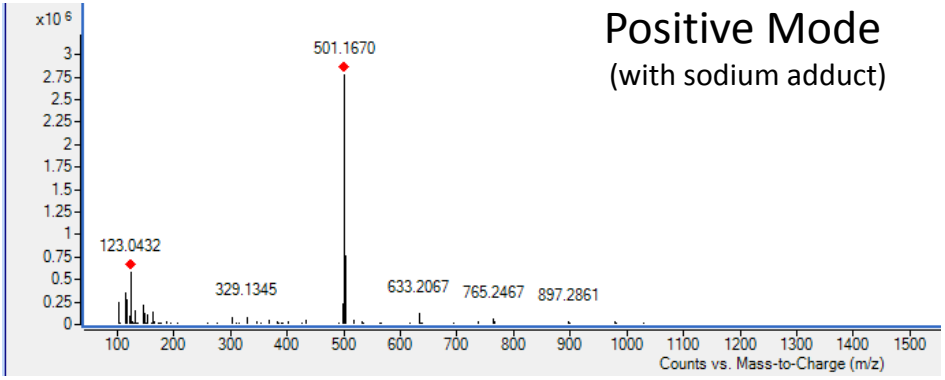

$C_{12}H_{14}O_3$

205.0943

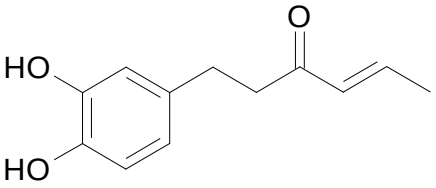

$C_7H_5O_2$

121.0290

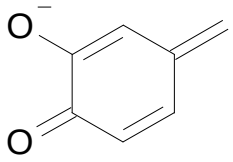

Negative Mode

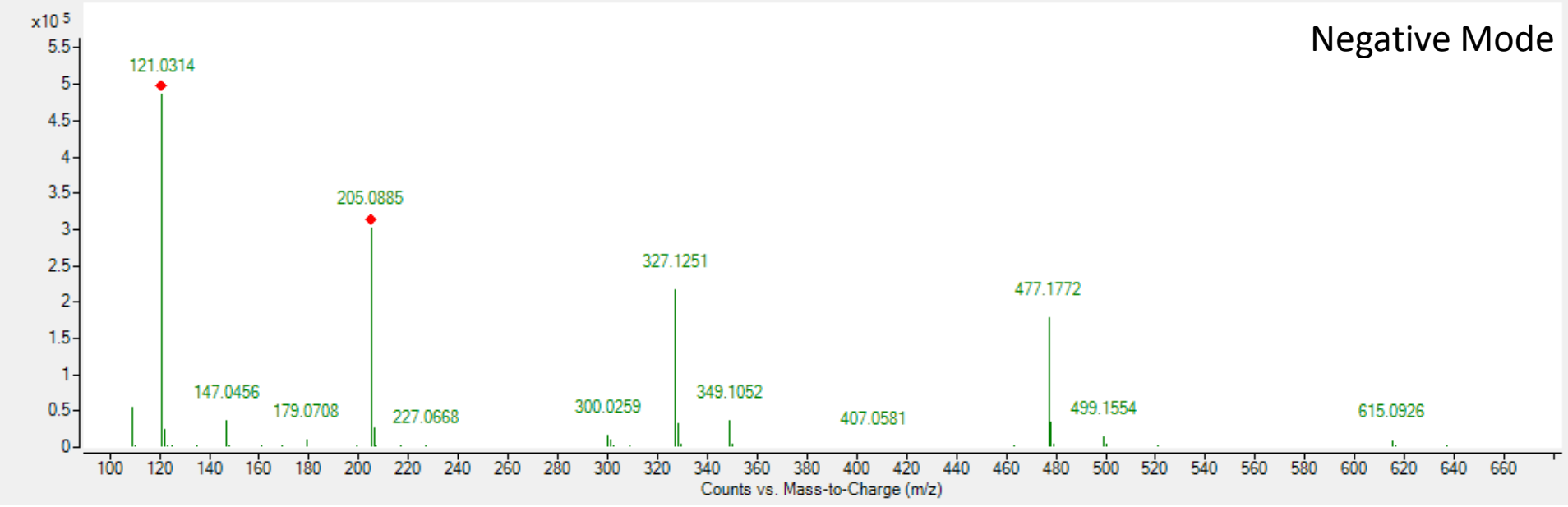

Peak # 24:

Related to Alnuside A with glucose

m/z 491.1925, $C_{25}H_{30}O_{10}$

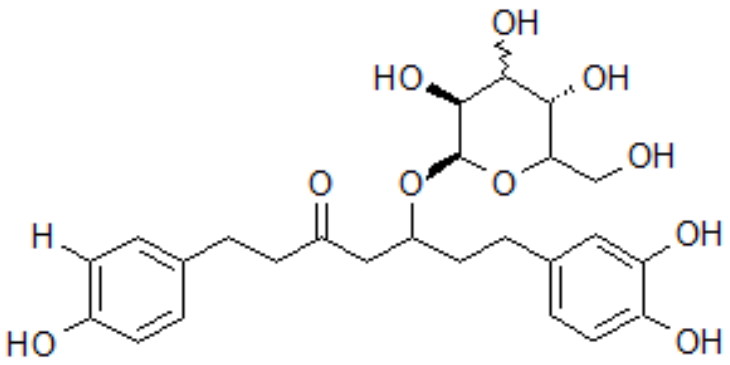

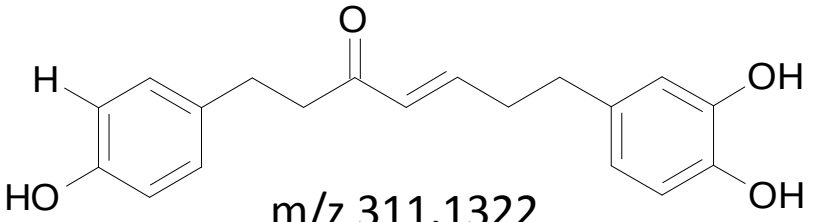

m/z 311.1322

$C_{19}H_{20}O_4$

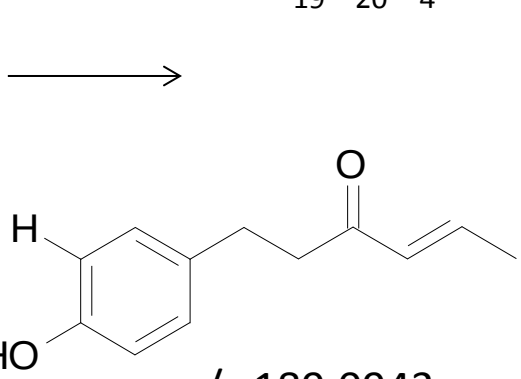

m/z 189.0943

$C_{12}H_{14}O_2$

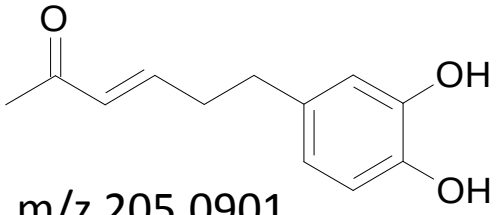

m/z 205.0901

$C_{12}H_{14}O_2$

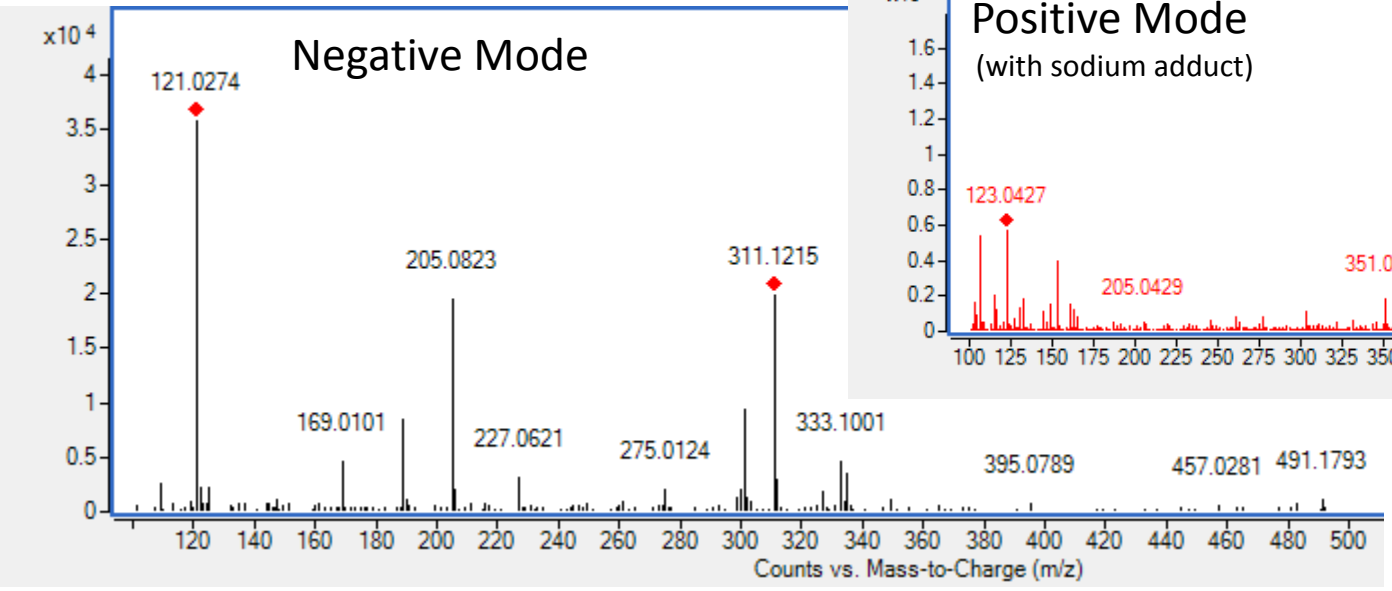

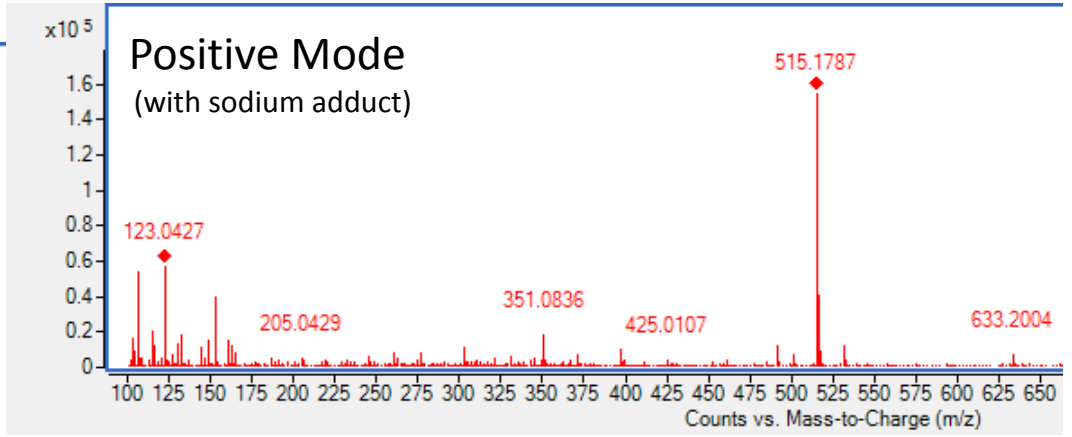

Peak # 25:

Quercitin glucuronide

m/z 477.0675, $C_{21}H_{18}O_{13}$

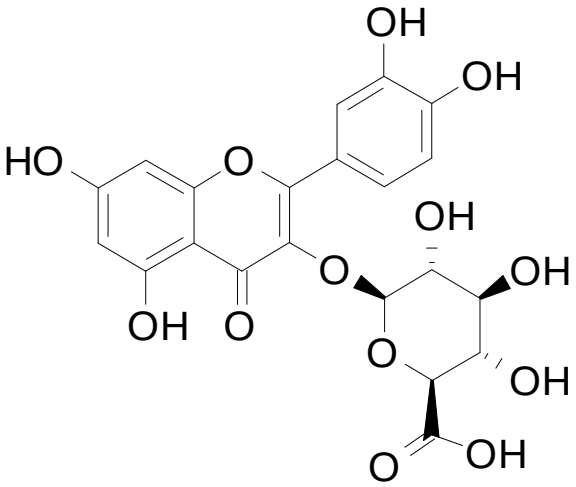

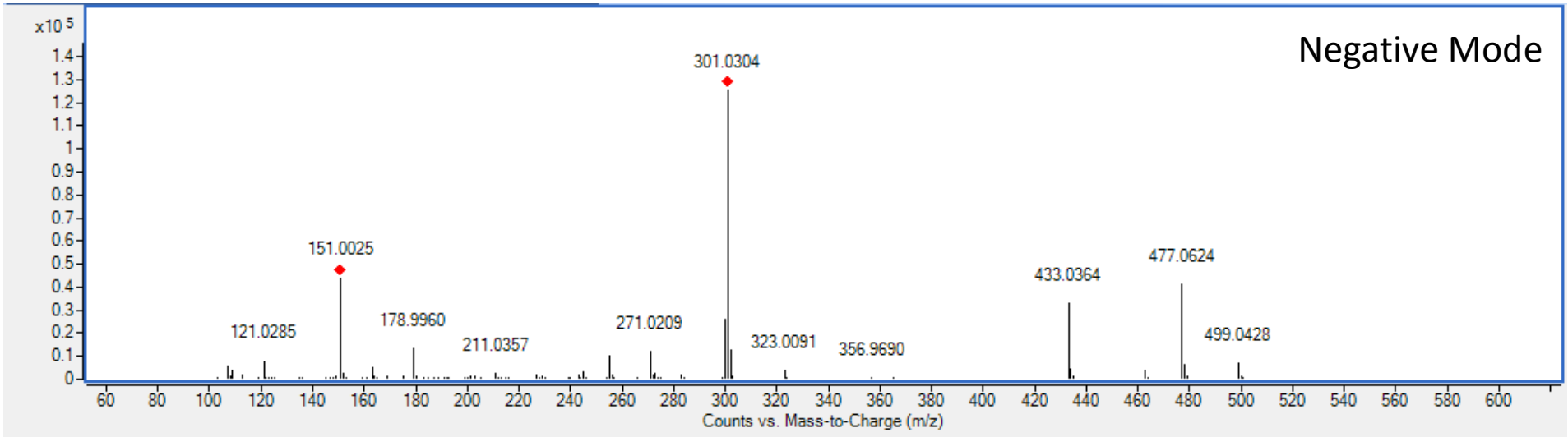

Peak # 25:

Quercetin3-O-glucoside

m/z 463.0882, $C_{21}H_{20}O_{12}$

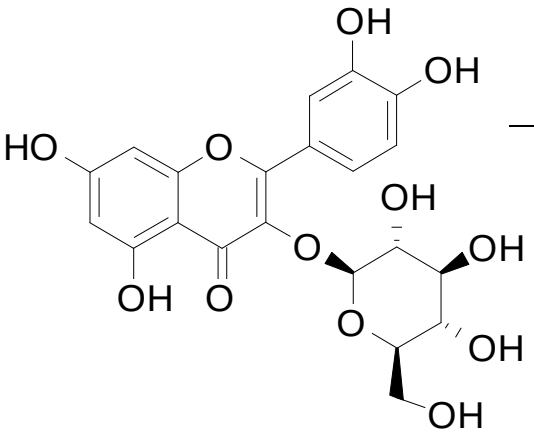

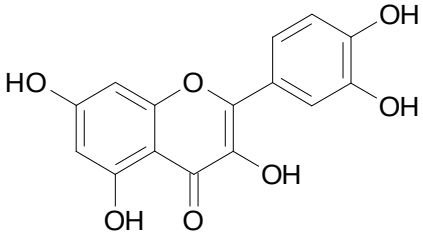

m/z- 301

$C_{15}H_{10}O_7$

$\downarrow -CH_2O$ $\downarrow -CO\text{-}CH_2$

m/z 271 m/z 255

$\downarrow -CO$ $\downarrow -CO$

m/z 243 m/z 227

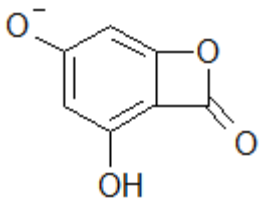

m/z 151

$C_7H_{30}O_4$

Xaio-qin et al 2009 Investigation of the chemical constituents and variation of the flower buds of Lonicera species by UPLC-ESI-MS/MS and principle component analysis. Act. Pharm Sin 44:895-904.

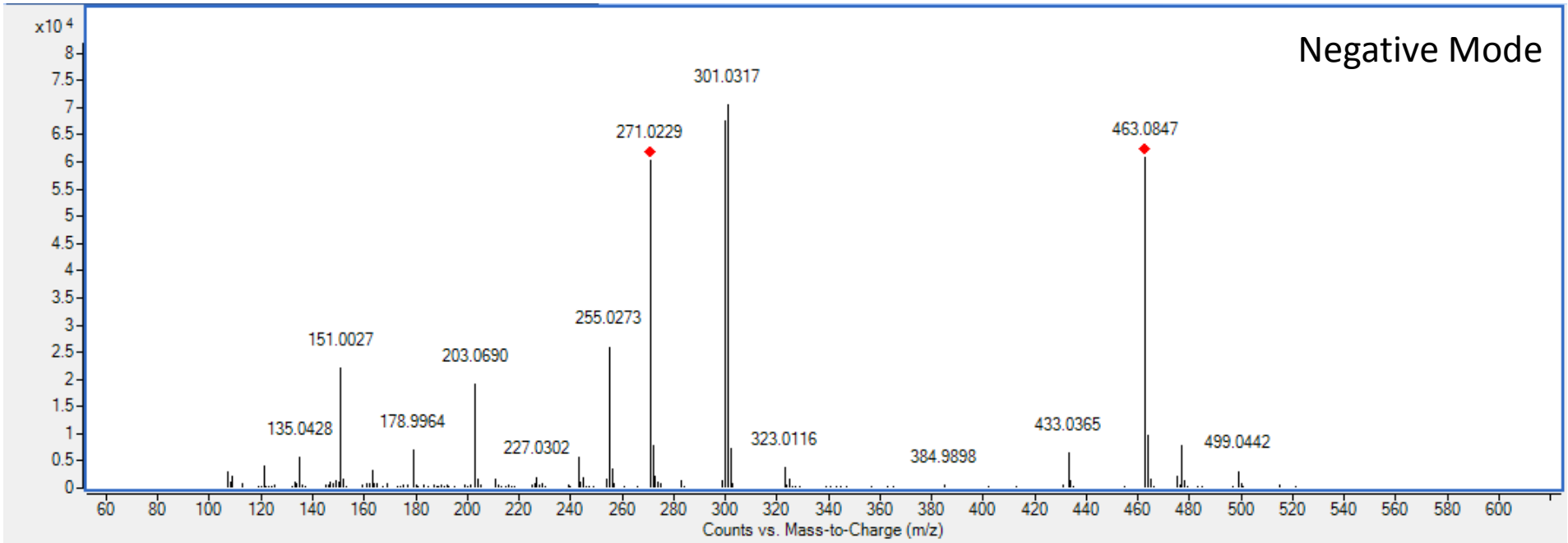

Peaks #26:
Alnuside A
m/z 461.1858, $C_{24}H_{30}O_9$

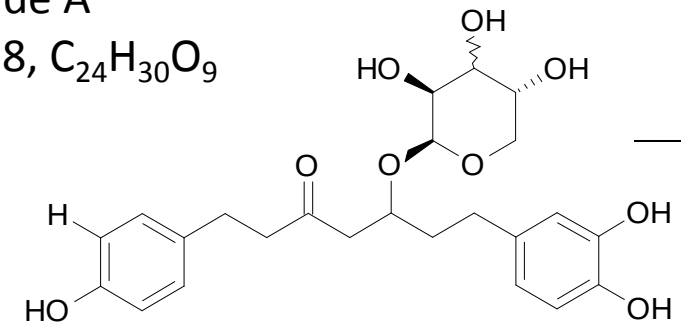

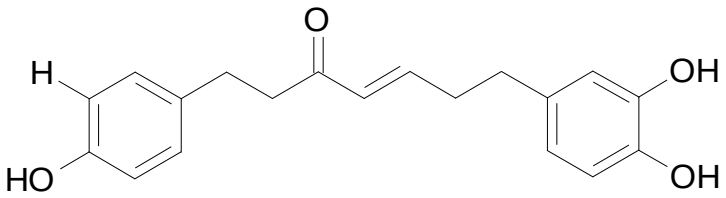

m/z 311.1322
$C_{19}H_{20}O_4$

Positive Mode
(with sodium adduct)

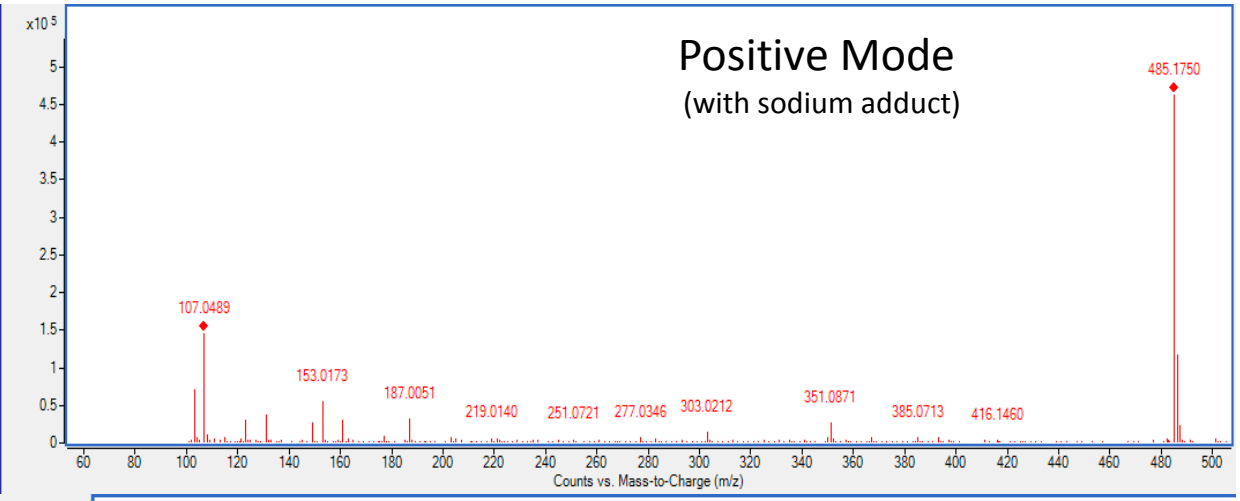

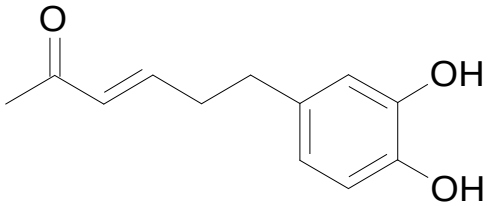

m/z 205.0901
$C_{12}H_{14}O_2$

Negative Mode

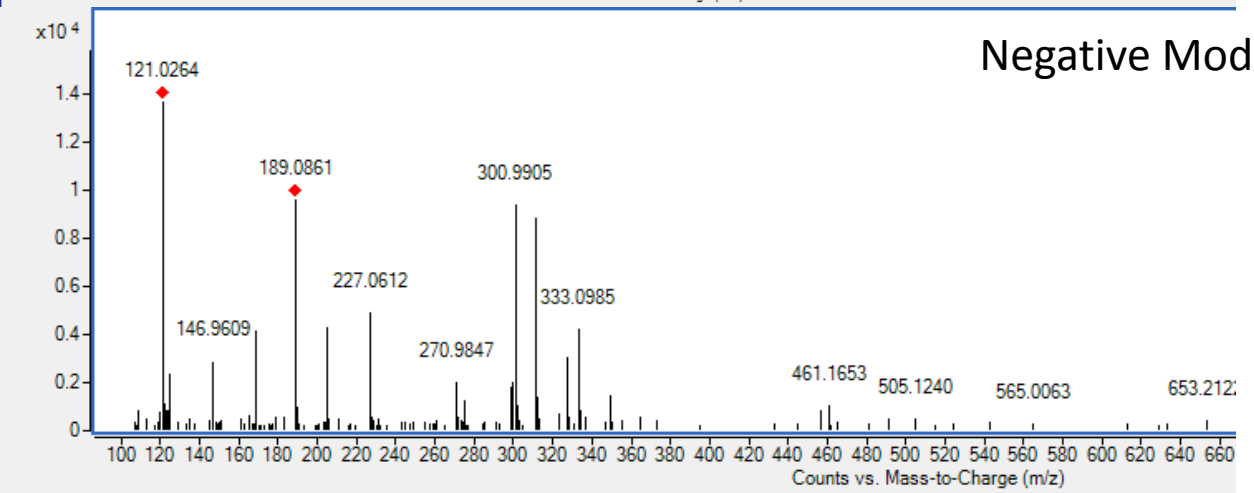

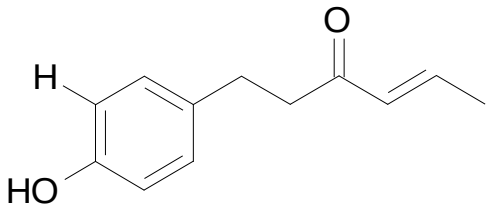

m/z 189.0943
$C_{12}H_{14}O_2$

Peaks #27:

Alnuside B

m/z 461.1858, $C_{24}H_{30}O_9$

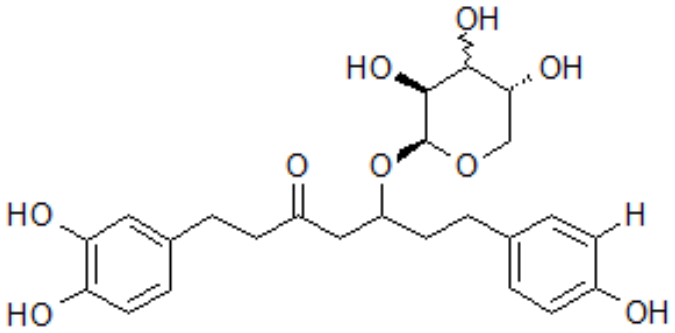

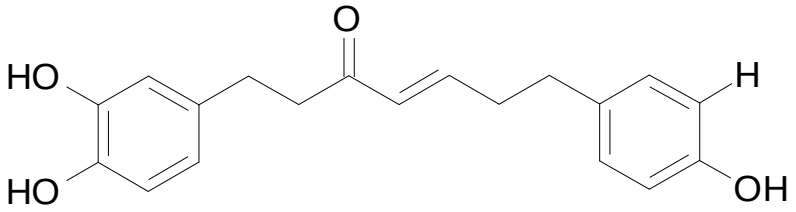

m/z 311.1322, $C_{19}H_{20}O_4$

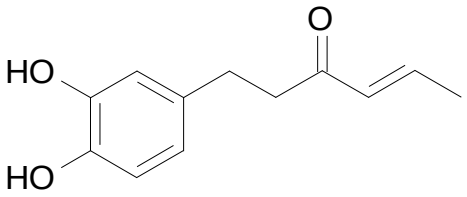

m/z 205.0901, $C_{12}H_{14}O_2$

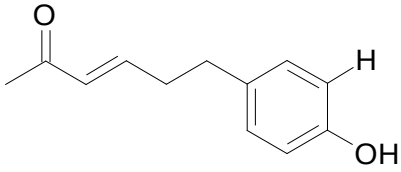

m/z 189.0943, $C_{12}H_{14}O_2$

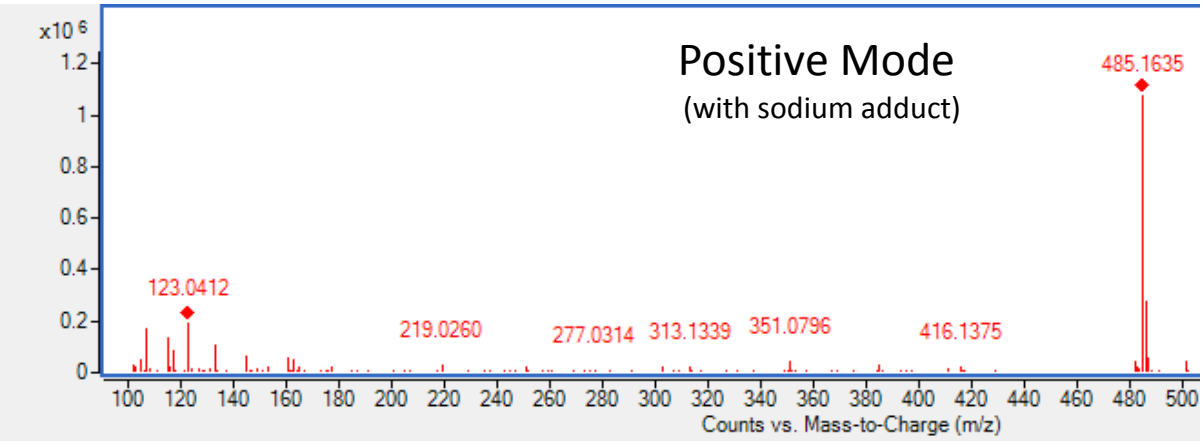

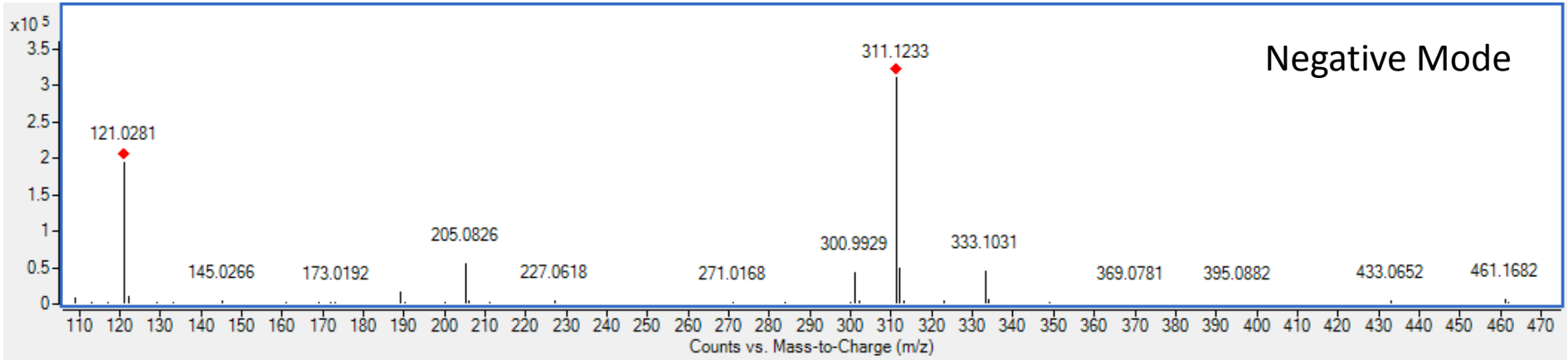

Peak # 29:
Quercitin rhamnoside
m/z 447.0964, $C_{21}H_{19}O_{11}$

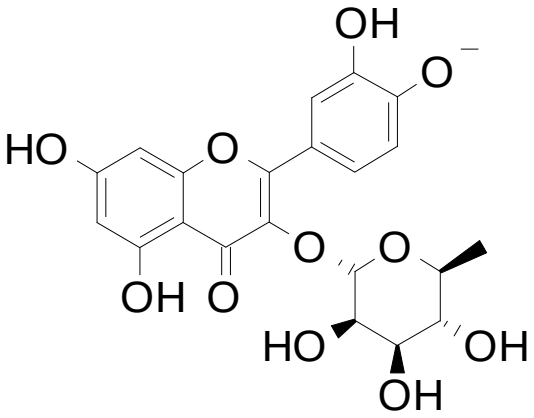

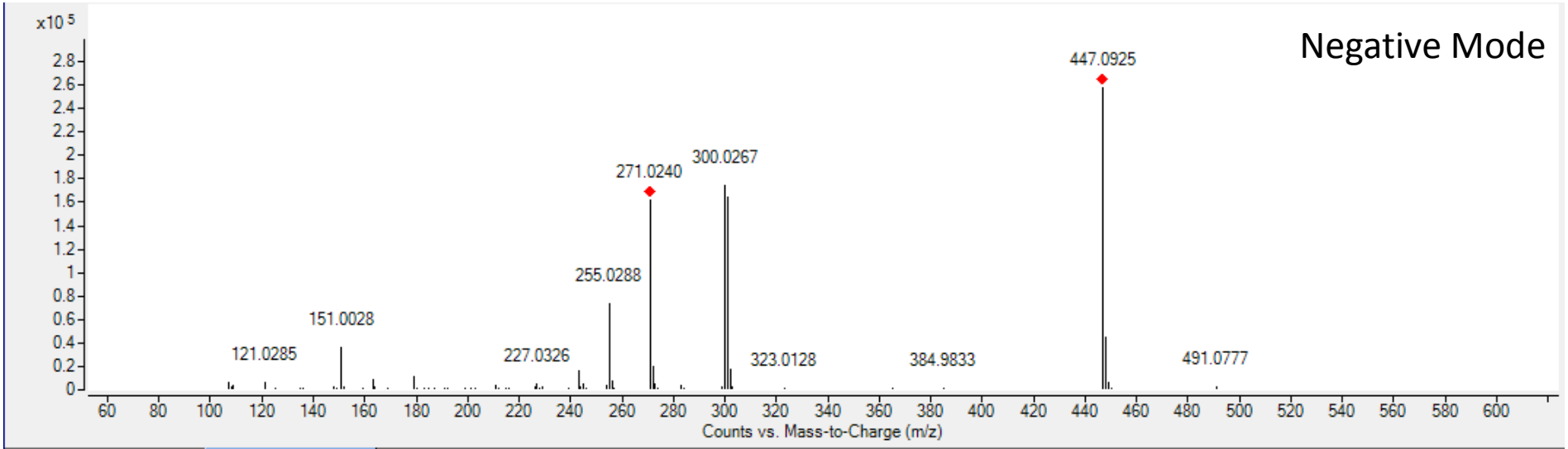

Peak # 30:
5(S)-methylhirsutanonol
m/z 359.1573, $C_{20}H_{24}O_6$

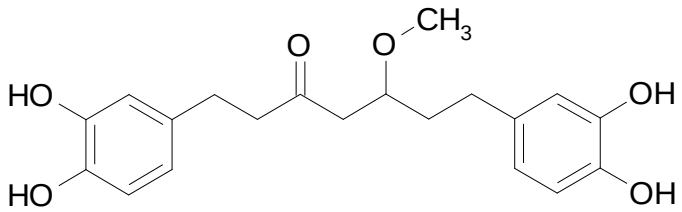

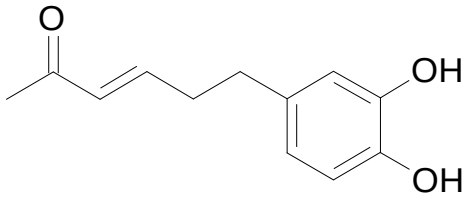

$C_{12}H_{14}O_3$
205.0943

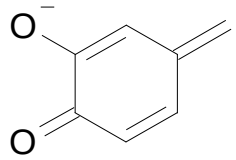

$C_7H_5O_2$
121.0290

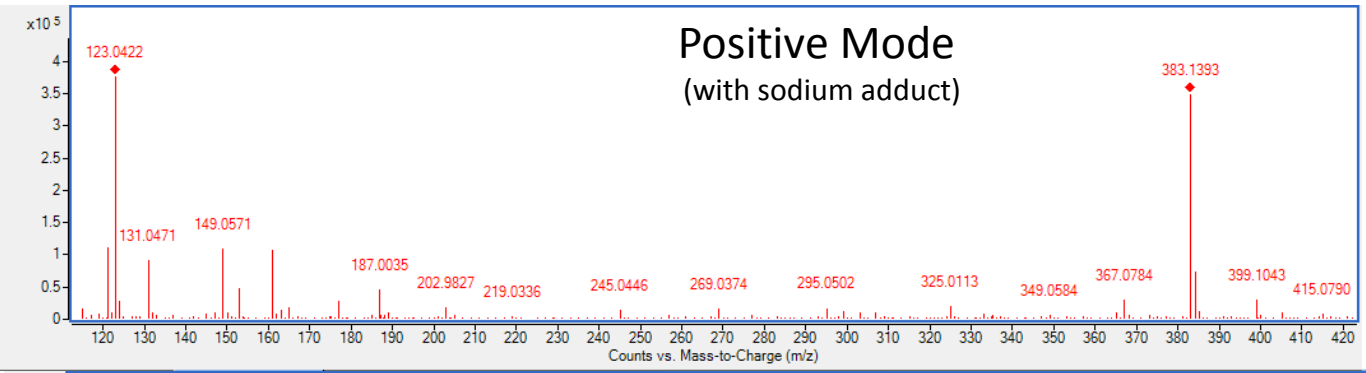

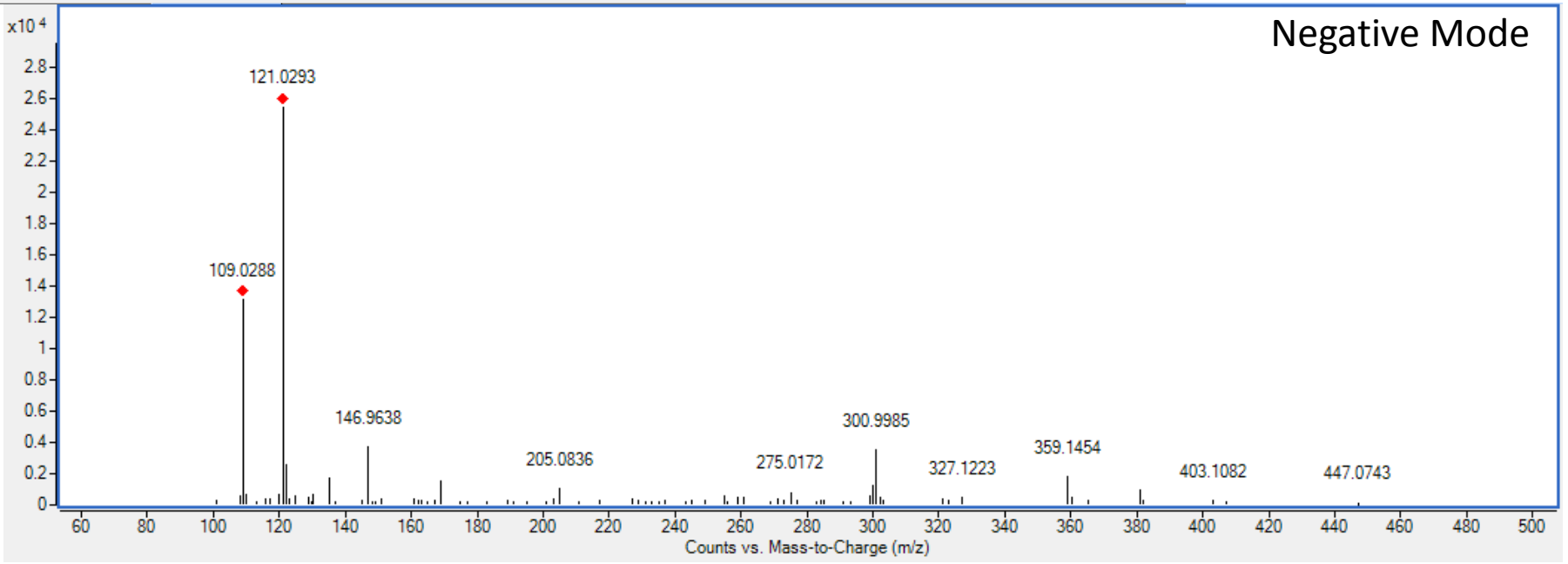

Peak # 31

platyphylanolonol-5-b-D-xylopyranoside

MW 445.1866, $C_{24}H_{30}O_8$

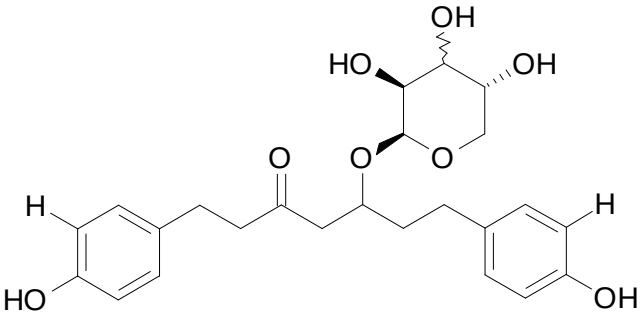

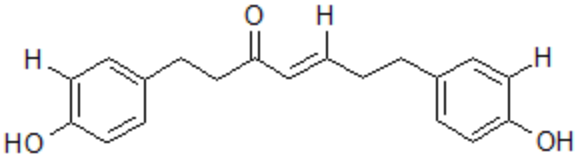

$C_{19}H_{20}O_3$

295

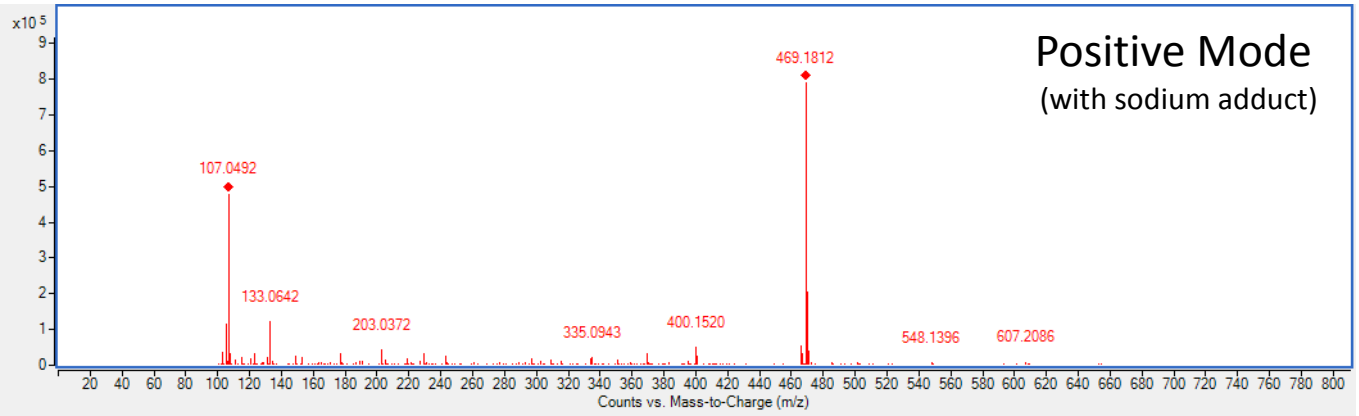

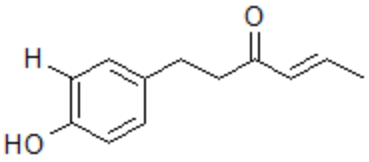

$C_{12}H_{14}O_2$

189

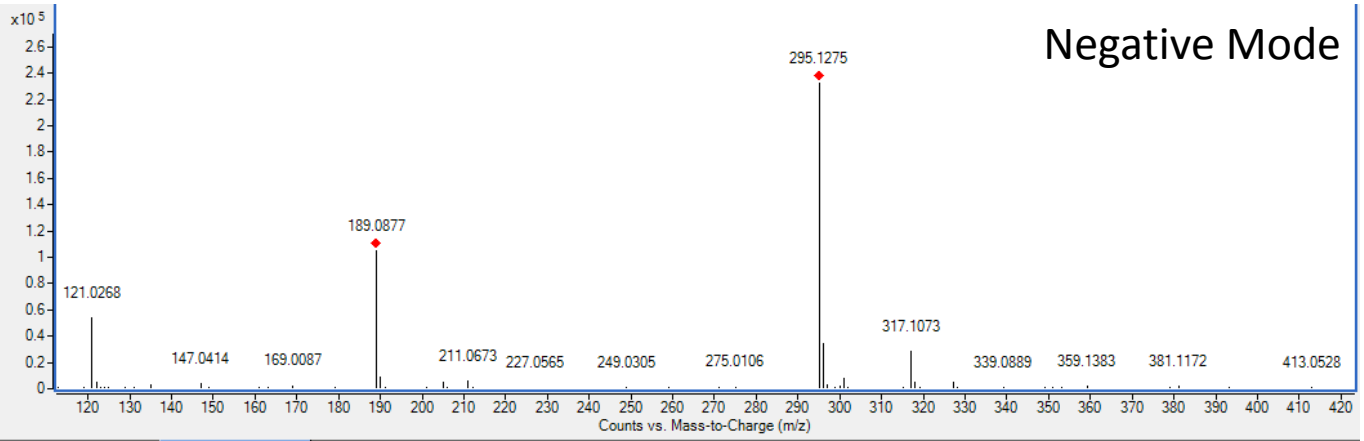

$C_7H_5O_2$

121.0290

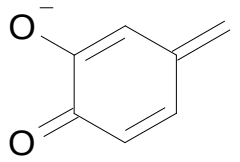

Peak # 32:
Hirsutanone
M-H 327.12379, $C_{19}H_{19}O_5$

$C_{19}H_{20}O_5$
327.1311

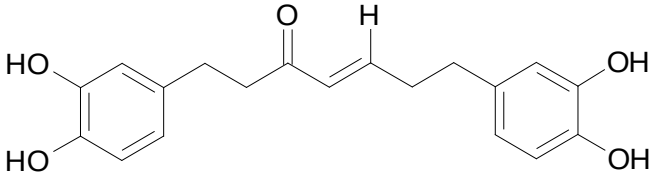

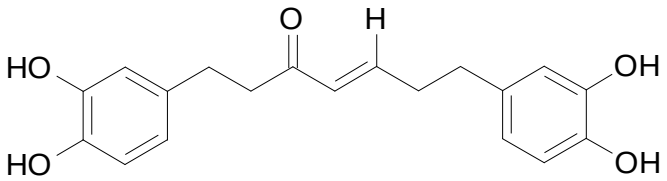

$C_{12}H_{14}O_3$
205.0943

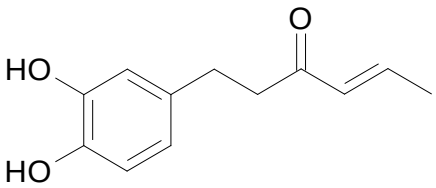

$C_7H_5O_2$
121.0290

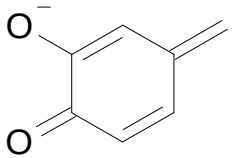

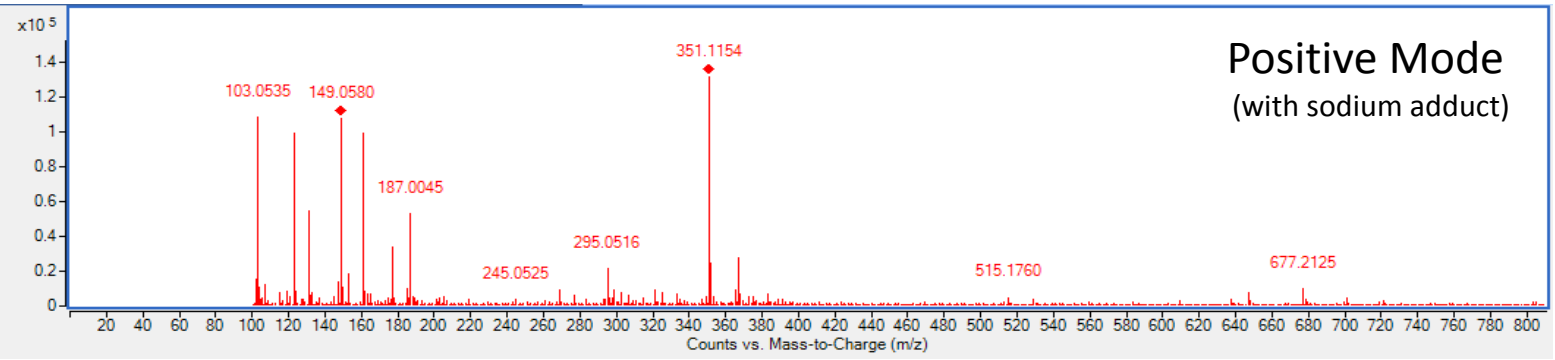

Positive Mode
(with sodium adduct)

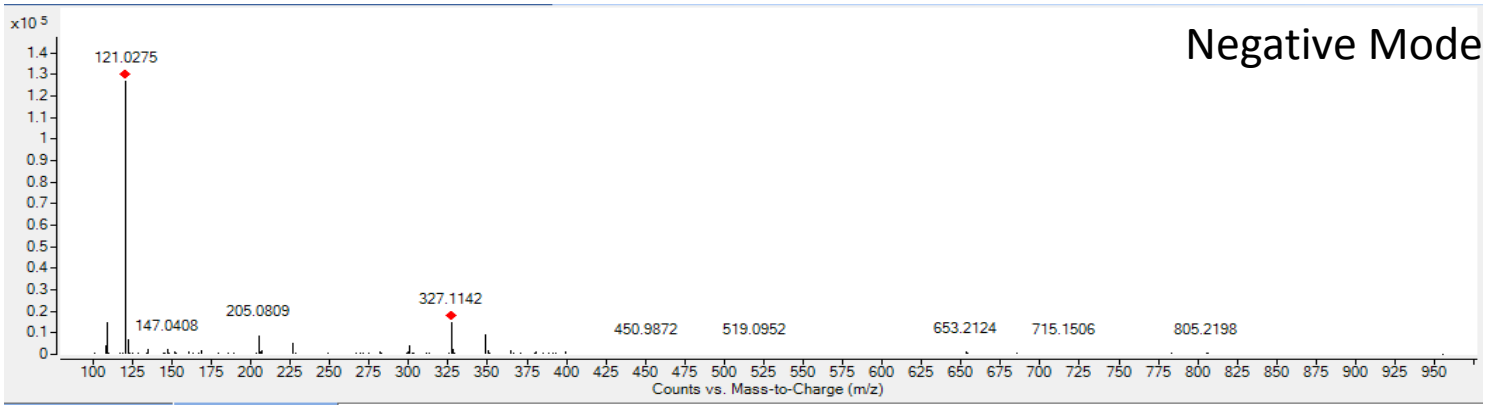

Negative Mode

Peak # 34:

derivative of Alnuside C with glucose replacing xylose

m/z 591.2520, $C_{30}H_{40}O_{12}$

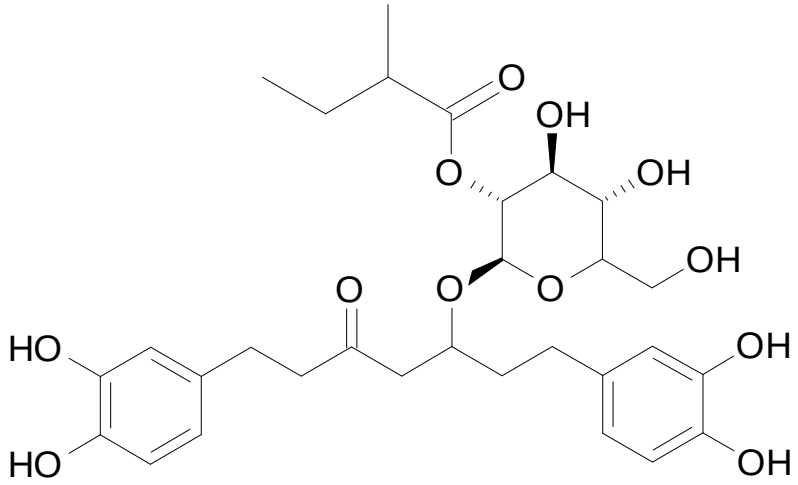

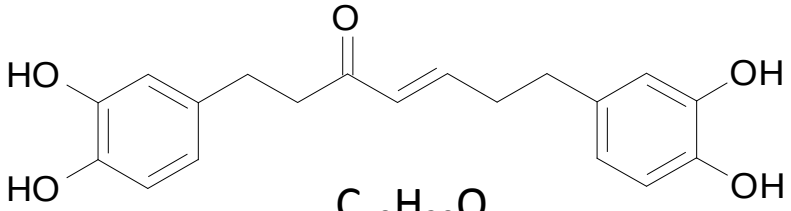

$C_{19}H_{20}O_5$

327.1311

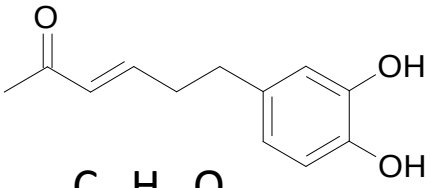

$C_{12}H_{14}O_3$

205.0943

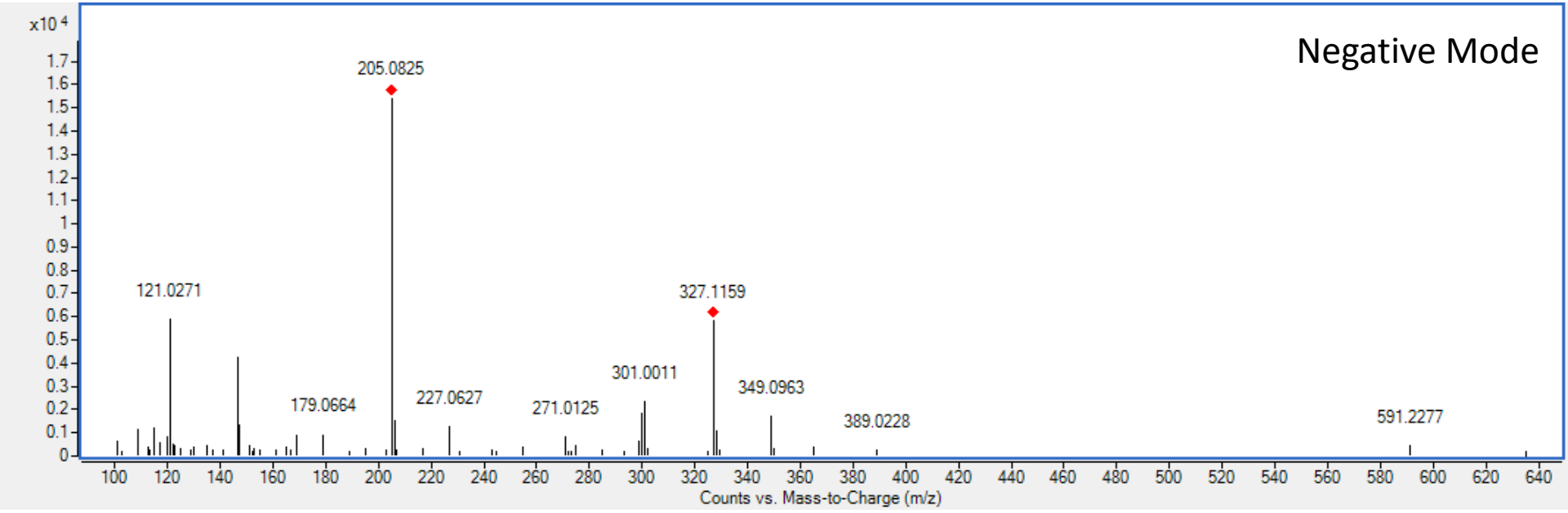

Peak # 35

Alnuside C

m/z 561.2414, $C_{29}H_{38}O_{11}$

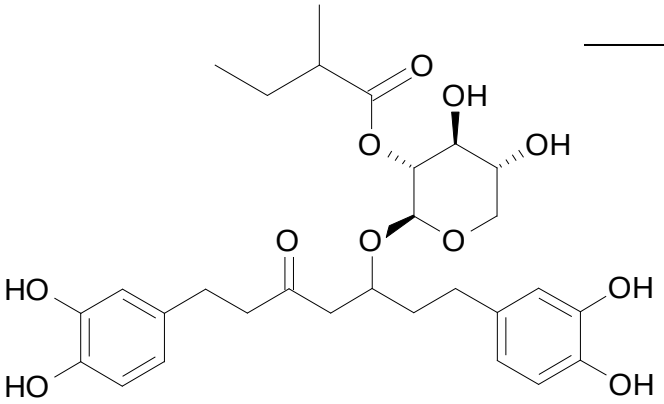

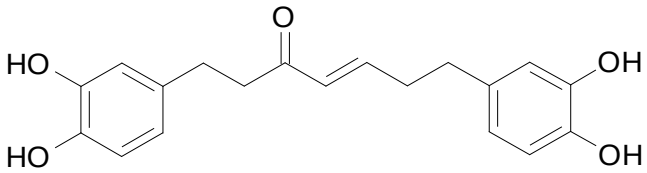

$C_{19}H_{20}O_5$

327.1311

$C_{12}H_{14}O_3$

205.0943

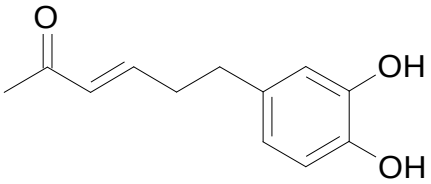

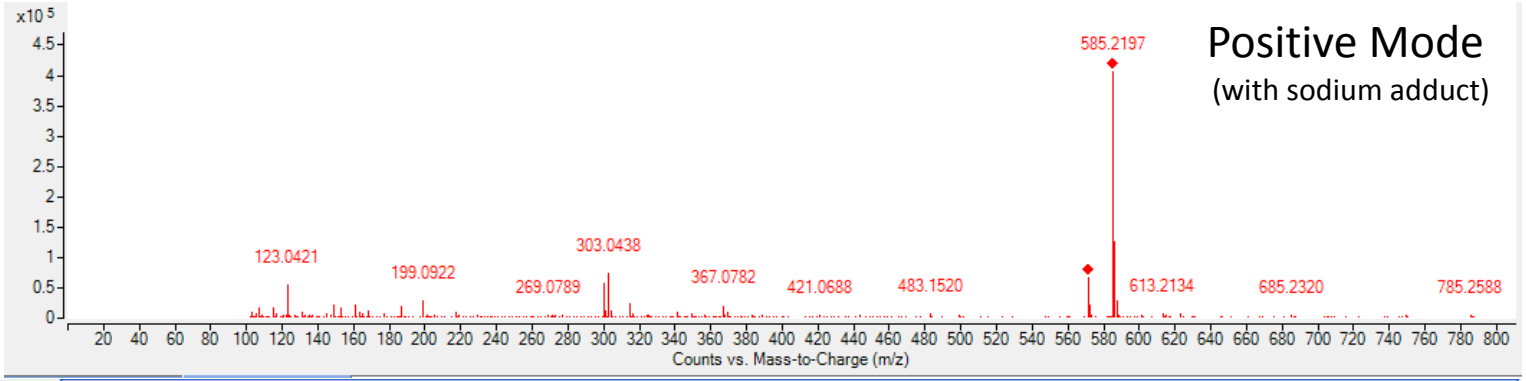

Positive Mode

(with sodium adduct)

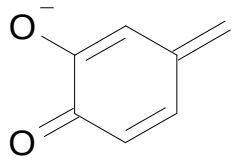

$C_7H_5O_2$

121.0290

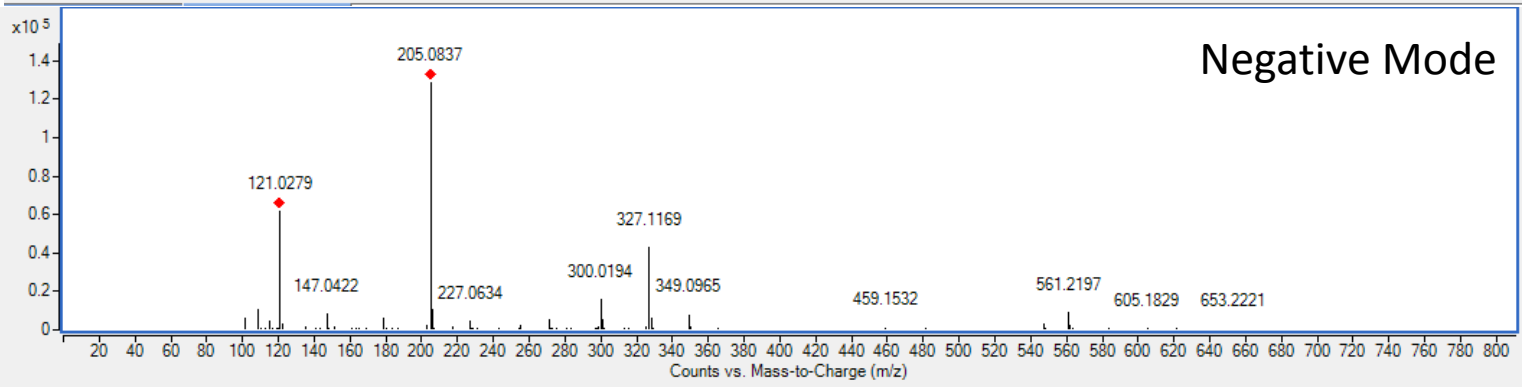

Negative Mode